
Distributed Stochastic Optimization of the Regularized Risk

Shin Matsushima*

University of Tokyo
Tokyo, Japan

shin.matsushima@mist.i.u-tokyo.ac.jp

Hyokun Yun

Purdue University
West Lafayette, IN

yun3@purdue.edu

S.V.N. Vishwanathan

Purdue University
West Lafayette, IN

vishy@stat.purdue.edu

Abstract

Many machine learning algorithms minimize a regularized risk, and stochastic optimization is widely used for this task. When working with massive data, it is desirable to perform stochastic optimization in parallel. Unfortunately, many existing stochastic algorithms cannot be parallelized efficiently. In this paper we show that one can rewrite the regularized risk minimization problem as an equivalent saddle-point problem, which is amenable for distributed stochastic optimization (DSO). We prove rates of convergence of our algorithm. DSO outperforms state-of-the-art algorithms when used for training linear support vector machines (SVMs) and logistic regression on the publicly available datasets.

1 Introduction

Regularized risk minimization is a well-known paradigm in machine learning [19]:

$$P(\mathbf{w}) = \lambda \sum_j \phi_j(w_j) + \frac{1}{m} \sum_{i=1}^m \ell(\langle \mathbf{w}, \mathbf{x}_i \rangle, y_i). \quad (1)$$

Here, we are given m training data points $\mathbf{x}_i \in \mathbb{R}^d$ and their corresponding labels y_i , while $\mathbf{w} \in \mathbb{R}^d$ is the parameter of the model. Furthermore, w_j denotes the j -th component of \mathbf{w} , while $\phi_j(\cdot)$ is a convex function which penalizes complex models. $\ell(\cdot, \cdot)$ is a loss function, which is convex in \mathbf{w} . Moreover, $\langle \cdot, \cdot \rangle$ denotes the Euclidean inner product, and $\lambda > 0$ is a scalar which trades-off between the average loss and the regularizer. For brevity, we will use $\ell_i(\langle \mathbf{w}, \mathbf{x}_i \rangle)$ to denote $\ell(\langle \mathbf{w}, \mathbf{x}_i \rangle, y_i)$.

Many well-known models can be derived by specializing (1). For instance, if $y_i \in \{\pm 1\}$, then setting $\phi_j(w_j) = w_j^2$ and $\ell_i(\langle \mathbf{w}, \mathbf{x}_i \rangle) = \max(0, 1 - y_i \langle \mathbf{w}, \mathbf{x}_i \rangle)$ recovers binary linear support vector machines (SVMs) [17]. On the other hand, using the same regularizer but changing the loss function to $\ell_i(\langle \mathbf{w}, \mathbf{x}_i \rangle) = \log(1 + \exp(-y_i \langle \mathbf{w}, \mathbf{x}_i \rangle))$ yields regularized logistic regression [8]. Similarly, setting $\ell_i(\langle \mathbf{w}, \mathbf{x}_i \rangle) = \frac{1}{2} (y_i - \langle \mathbf{w}, \mathbf{x}_i \rangle)^2$ and $\phi_j(w_j) = |w_j|$ leads to LASSO [8].

A number of specialized as well as general purpose algorithms have been proposed for minimizing the regularized risk. For instance, if both the loss and the regularizer are smooth, as is the case with logistic regression, then quasi-Newton algorithms such as L-BFGS [11] have been found to be very successful. On the other hand, for smooth regularizers but non-smooth loss functions, Teo et al. [19]

*Part of the research was performed when visiting Purdue University.

proposed a bundle method for regularized risk minimization (BMRM). Both L-BFGS and BMRM belong to the broad class of batch minimization algorithms. That is, in order to perform a parameter update, at every iteration these algorithms compute the regularized risk $P(\mathbf{w})$ as well as its gradient

$$\nabla P(\mathbf{w}) = \lambda \sum_{j=1}^d \nabla \phi_j(w_j) \cdot \mathbf{e}_j + \frac{1}{m} \sum_{i=1}^m \nabla \ell_i(\langle \mathbf{w}, \mathbf{x}_i \rangle) \cdot \mathbf{x}_i, \quad (2)$$

where \mathbf{e}_j denotes the j -th standard basis vector. Both $P(\mathbf{w})$ as well as the gradient $\nabla P(\mathbf{w})$ take $O(md)$ time to compute, which is computationally expensive when m , the number of data points, is large. Batch algorithms overcome this hurdle by using the fact that the empirical risk $\frac{1}{m} \sum_{i=1}^m \ell_i(\langle \mathbf{w}, \mathbf{x}_i \rangle)$ as well as its gradient $\frac{1}{m} \sum_{i=1}^m \nabla \ell_i(\langle \mathbf{w}, \mathbf{x}_i \rangle) \cdot \mathbf{x}_i$ decompose over the data points, and therefore one can compute $P(\mathbf{w})$ and $\nabla P(\mathbf{w})$ in a distributed fashion [4].

Batch algorithms, unfortunately, are known to be unfavorable for large scale machine learning both empirically and theoretically [2]. It is now widely accepted that stochastic algorithms which process one data point at a time are more effective for regularized risk minimization. In a nutshell, the idea here is that (2) can be stochastically approximated by

$$\mathbf{g}_i = \lambda \sum_{j=1}^d \nabla \phi_j(w_j) \cdot \mathbf{e}_j + \nabla \ell_i(\langle \mathbf{w}, \mathbf{x}_i \rangle) \cdot \mathbf{x}_i, \quad (3)$$

when i is chosen uniformly random in $\{1, \dots, m\}$. Since \mathbf{g}_i is an unbiased estimator of the true gradient $\nabla P(\mathbf{w})$, we have that $\nabla P(\mathbf{w}) = \mathbb{E}_{i \in \{1, \dots, m\}} [\mathbf{g}_i]$. Now we can replace the true gradient by this *stochastic* gradient to rewrite a gradient descent update as

$$\mathbf{w} \leftarrow \mathbf{w} - \eta \cdot \mathbf{g}_i. \quad (4)$$

Computing \mathbf{g}_i only takes $O(d)$ effort, which is independent of m , the number of data points. Bottou and Bousquet [2] show that stochastic optimization is asymptotically faster than gradient descent and the other second-order methods such as L-BFGS for regularized risk minimization.

However, a drawback of update (4) is that it is not easy to parallelize. There are two main difficulties: computing \mathbf{g}_i (3) requires *reading* the latest value of \mathbf{w} , while updating (4) requires *writing* to the components of \mathbf{w} . Existing parallel stochastic optimization algorithms try to work around these difficulties in a somewhat ad-hoc manner (see Section 4). In this paper, we take a fundamentally different approach and propose a reformulation of the regularized risk (1), for which one can *naturally* derive a parallel stochastic optimization algorithm. Our technical contributions are:

- We reformulate regularized risk minimization as an equivalent saddle-point problem, and show that it can be solved via distributed stochastic optimization (DSO).
- We prove $O(1/\sqrt{T})$ rates of convergence for DSO, and show that it scales almost linearly with the number of processors.
- We verify that when used for training linear support vector machines (SVMs) or binary logistic regression, DSO outperforms general-purpose stochastic (*e.g.*, [22]) or batch (*e.g.*, [19]) optimizers on the publicly available datasets.

2 Reformulating Regularized Risk Minimization

We begin by reformulating the regularized risk minimization problem as an equivalent saddle-point problem. Towards this end, we first rewrite (1) by introducing an auxiliary variable u_i for each data point:

$$\min_{\mathbf{w}, \mathbf{u}} \lambda \sum_{j=1}^d \phi_j(w_j) + \frac{1}{m} \sum_{i=1}^m \ell_i(u_i) \quad (5a)$$

$$\text{s.t. } u_i = \langle \mathbf{w}, \mathbf{x}_i \rangle \quad \forall i = 1, \dots, m. \quad (5b)$$

By introducing Lagrange multipliers α_i to eliminate the constraints, we obtain

$$\min_{\mathbf{w}, \mathbf{u}} \max_{\boldsymbol{\alpha}} \lambda \sum_{j=1}^d \phi_j(w_j) + \frac{1}{m} \sum_{i=1}^m \ell_i(u_i) + \frac{1}{m} \sum_{i=1}^m \alpha_i (u_i - \langle \mathbf{w}, \mathbf{x}_i \rangle).$$

Name	$\ell_i(u)$	$-\ell_i^*(-\alpha)$
Hinge	$\max(1 - y_i u, 0)$	$y_i \alpha$ for $\alpha \in [0, y_i]$
Logistic	$\log(1 + \exp(-y_i u))$	$-\{y_i \alpha \log(y_i \alpha) + (1 - y_i \alpha) \log(1 - y_i \alpha)\}$ for $\alpha \in (0, y_i)$
Square	$(u - y_i)^2/2$	$y_i \alpha - \alpha^2/2$

Table 1: Different loss functions and their duals. $[0, y_i]$ denotes $[0, 1]$ if $y_i = 1$, and $[-1, 0]$ if $y_i = -1$; $(0, y_i)$ is defined similarly.

Here \mathbf{u} denotes a vector whose components are u_i . Likewise, α is a vector whose components are α_i . Since the objective function (5) is convex and the constraints are linear, strong duality applies [3]. Therefore, we can switch the maximization over α and the minimization over \mathbf{w}, \mathbf{u} :

$$\max_{\alpha} \min_{\mathbf{w}, \mathbf{u}} \lambda \sum_{j=1}^d \phi_j(w_j) + \frac{1}{m} \sum_{i=1}^m \ell_i(u_i) + \frac{1}{m} \sum_{i=1}^m \alpha_i (u_i - \langle \mathbf{w}, \mathbf{x}_i \rangle).$$

Grouping terms which depend only on \mathbf{u} yields

$$\max_{\alpha} \min_{\mathbf{w}, \mathbf{u}} \lambda \sum_{j=1}^d \phi_j(w_j) - \frac{1}{m} \sum_{i=1}^m \alpha_i \langle \mathbf{w}, \mathbf{x}_i \rangle + \frac{1}{m} \sum_{i=1}^m \alpha_i u_i + \ell_i(u_i).$$

Note that the first two terms in the above equation are independent of \mathbf{u} , and $\min_{u_i} \alpha_i u_i + \ell_i(u_i)$ is $-\ell_i^*(-\alpha_i)$ where $\ell_i^*(\cdot)$ is the Fenchel-Legendre conjugate of $\ell_i(\cdot)$ [3] (see Table 1 for some examples). The above transformations yield to our final objective function:

$$\max_{\alpha} \min_{\mathbf{w}} f(\mathbf{w}, \alpha) := \lambda \sum_{j=1}^d \phi_j(w_j) - \frac{1}{m} \sum_{i=1}^m \alpha_i \langle \mathbf{w}, \mathbf{x}_i \rangle - \frac{1}{m} \sum_{i=1}^m \ell_i^*(-\alpha_i).$$

If we take the gradient of $f(\mathbf{w}, \alpha)$ in terms of \mathbf{w} and set it to zero to eliminate \mathbf{w} , then we obtain the so-called dual objective which is a function of α . Moreover, any \mathbf{w}^* which is a solution of the primal problem (1), and any α^* which is a solution of the dual problem is a saddle point of $f(\mathbf{w}, \alpha)$ [3]. In other words, minimizing the primal, maximizing the dual, and finding a saddle point of $f(\mathbf{w}, \alpha)$ are all equivalent problems.

2.1 Stochastic Optimization

Let x_{ij} denote the j -th coordinate of \mathbf{x}_i , and $\Omega_i := \{j : x_{ij} \neq 0\}$ denote the non-zero coordinates of \mathbf{x}_i . Similarly, let $\bar{\Omega}_j := \{i : x_{ij} \neq 0\}$ denote the set of data points where the j -th coordinate is non-zero and $\Omega := \{(i, j) : x_{ij} \neq 0\}$ denotes the set of all non-zero coordinates in the training dataset $\mathbf{x}_1, \dots, \mathbf{x}_m$. Then, $f(\mathbf{w}, \alpha)$ can be rewritten as

$$f(\mathbf{w}, \alpha) = \sum_{(i,j) \in \Omega} \underbrace{\frac{\lambda \phi_j(w_j)}{|\bar{\Omega}_j|} - \frac{\ell_i^*(-\alpha_i)}{m |\Omega_i|} - \frac{\alpha_i w_j x_{ij}}{m}}_{f_{i,j}(w_j, \alpha_i)} := \sum_{(i,j) \in \Omega} f_{i,j}(w_j, \alpha_i), \quad (6)$$

where $|\cdot|$ denotes the cardinality of a set. Remarkably, each component $f_{i,j}$ in the above summation depends only on one component w_j of \mathbf{w} and one component α_i of α . This allows us to derive an optimization algorithm which is stochastic in terms of both i and j . Let us define

$$\mathbf{g}_{i,j} := \left(|\Omega| \left(\frac{\lambda \nabla \phi_j(w_j)}{|\bar{\Omega}_j|} - \frac{\alpha_i x_{ij}}{m} \right) \mathbf{e}_j, |\Omega| \left(-\frac{\nabla \ell_i^*(-\alpha_i)}{m |\Omega_i|} - \frac{w_j x_{ij}}{m} \right) \mathbf{e}_i \right). \quad (7)$$

Under the uniform distribution over $(i, j) \in \Omega$, one can easily see that $\mathbf{g}_{i,j}$ is an unbiased estimate of the gradient of $f(\mathbf{w}, \alpha)$, that is, $(\nabla_{\mathbf{w}} f(\mathbf{w}, \alpha), -\nabla_{\alpha} f(\mathbf{w}, \alpha)) = \mathbb{E}_{\{(i,j) \in \Omega\}} [\mathbf{g}_{i,j}]$. Since we are interested in finding a saddle point of $f(\mathbf{w}, \alpha)$, our stochastic optimization algorithm uses the stochastic gradient $\mathbf{g}_{i,j}$ to take a *descent* step in \mathbf{w} and an *ascent* step in α [14]:

$$w_j \leftarrow w_j - \eta \cdot \left(\frac{\lambda \nabla \phi_j(w_j)}{|\bar{\Omega}_j|} - \frac{\alpha_i x_{ij}}{m} \right), \text{ and } \alpha_i \leftarrow \alpha_i + \eta \cdot \left(-\frac{\nabla \ell_i^*(-\alpha_i)}{m |\Omega_i|} - \frac{w_j x_{ij}}{m} \right). \quad (8)$$

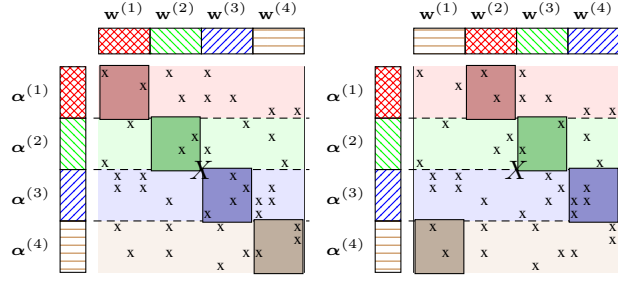


Figure 1: Illustration of DSO with 4 processors. The rows of the data matrix X as well as the parameters \mathbf{w} and α are partitioned as shown. Colors denote ownerships. The active area of each processor is in dark colors. Left: the initial state. Right: the state after one bulk synchronization.

Note that in the above discussion, we implicitly assumed that $\phi_j(\cdot)$ and $\ell_i^*(\cdot)$ are differentiable. If that is not the case, then their derivatives can be replaced by sub-gradients [3]. Nemirovski et al. [14] proved that under mild technical conditions (all of which our objective function satisfies), the above stochastic procedure is guaranteed to converge to the saddle point of $f(\mathbf{w}, \alpha)$.

3 Parallelization

The minimax formulation (6) not only admits an efficient stochastic optimization algorithm, but also allows us to derive a distributed stochastic optimization (DSO) algorithm. The key observation underlying DSO is the following: Given (i, j) and (i', j') both in Ω , if $i \neq i'$ and $j \neq j'$ then one can simultaneously perform update (8) on (w_j, α_i) and $(w_{j'}, \alpha_{i'})$. In other words, the updates to w_j and α_j are independent of the updates to $w_{j'}$ and $\alpha_{i'}$, as long as $i \neq i'$ and $j \neq j'$.

Before we formally describe DSO we would like to present some intuition using Figure 1. Here we assume that we have 4 processors. The data matrix X is an $m \times d$ matrix formed by stacking \mathbf{x}_i^\top for $i = 1, \dots, m$, while \mathbf{w} and α denote the parameters to be optimized. The non-zero entries of X are marked by 'x's. Initially, both parameters as well as rows of the data matrix are partitioned across processors as depicted in Figure 1 (left); colors in the figure denote ownership *e.g.*, the first processor owns a fraction of the data matrix and a fraction of the parameters α and \mathbf{w} (denoted as $\mathbf{w}^{(1)}$ and $\alpha^{(1)}$) shaded with red. Each processor samples a non-zero entry x_{ij} of X within the dark shaded rectangular region (active area) depicted in the figure, and updates the corresponding w_j and α_i . After performing a fixed number of updates, the processors perform a bulk synchronization step and exchange coordinates of \mathbf{w} . This defines an inner iteration. After each inner iteration, ownership of the \mathbf{w} variables and hence the active area change, as shown in Figure 1 (right). If there are p processors, then p inner iterations define an epoch. Each coordinate of \mathbf{w} is updated by each processor at least once in an epoch. The algorithm iterates over epochs until convergence.

Three points are worth noting. First, since the active area of each processor does not share either row or column coordinates with the active area of other processors, as per our key observation above, the updates can be carried out by each processor in parallel without the need to communicate or synchronize with other processors. Second, we partition and distribute the data only once. The coordinates of α are partitioned at the beginning and are not exchanged by the processors. Only the coordinates of \mathbf{w} are exchanged after each bulk synchronization step. This means that there is very little communication overhead in our algorithm. Third, our algorithm can work in both shared memory as well as distributed memory setting. In the shared memory case the processors are threads and in the distributed memory case they are individual machines. In fact, we can also utilize a hybrid architecture, that is, multiple threads on multiple machines.

To formally describe DSO, suppose p processors are available, and let I_1, \dots, I_p denote p partitions of the set $\{1, \dots, m\}$ and J_1, \dots, J_p denote p partitions of the set $\{1, \dots, d\}$ such that $|I_q| \approx |I_{q'}|$ and $|J_r| \approx |J_{r'}|$. We partition the data $\{\mathbf{x}_1, \dots, \mathbf{x}_m\}$ and the labels $\{y_1, \dots, y_m\}$ into p disjoint subsets according to I_1, \dots, I_p and distribute them to p processors. The parameters $\{\alpha_1, \dots, \alpha_m\}$ are partitioned into p disjoint subsets $\alpha^{(1)}, \dots, \alpha^{(p)}$ according to I_1, \dots, I_p while $\{w_1, \dots, w_d\}$ are partitioned into p disjoint subsets $\mathbf{w}^{(1)}, \dots, \mathbf{w}^{(p)}$ according to J_1, \dots, J_p and distributed to p

processors. The partitioning of $\{1, \dots, m\}$ and $\{1, \dots, d\}$ induces a $p \times p$ partition of Ω :

$$\Omega^{(q,r)} := \{(i, j) \in \Omega : i \in I_q, j \in J_r\}, \quad q, r \in \{1, \dots, p\}.$$

The execution of DSO proceeds in epochs, and each epoch consists of p inner iterations; at the beginning of the r -th inner iteration ($r \geq 1$), processor q owns $\mathbf{w}^{(\sigma_r(q))}$ where $\sigma_r(q) = \{(q + r - 2) \bmod p\} + 1$, and executes stochastic updates (8) on coordinates in $\Omega^{(q, \sigma_r(q))}$. Since these updates only involve variables in $\alpha^{(q)}$ and $\mathbf{w}^{(\sigma_r(q))}$, no communication between processors is required to execute them. After every processor has finished a pre-defined number of updates, $\mathbf{w}^{(\sigma_r(q))}$ is sent to machine $\sigma_{r+1}^{-1}(\sigma_r(q))$ and the algorithm moves on to the $(r + 1)$ -st inner iteration. Detailed pseudo-code can be found in Algorithm 1.

Algorithm 1 Distributed stochastic optimization (DSO) for finding saddle point of (6)

```

1: Each processor  $q \in \{1, 2, \dots, p\}$  initializes  $\mathbf{w}^{(q)}, \alpha^{(q)}$ 
2:  $t \leftarrow 1$ 
3: repeat
4:    $\eta_t \leftarrow \eta_0 / \sqrt{t}$ 
5:   for all  $r \in \{1, 2, \dots, p\}$  do
6:     for all processors  $q \in \{1, 2, \dots, p\}$  in parallel do
7:       for  $(i, j) \in \Omega^{(q, \sigma_r(q))}$  do
8:          $w_j \leftarrow w_j - \eta_t \cdot \left( \frac{\lambda \nabla \phi_j(w_j)}{|\bar{\Omega}_j|} - \frac{\alpha_i x_{ij}}{m} \right)$  and  $\alpha_i \leftarrow \alpha_i + \eta_t \cdot \left( -\frac{\nabla \ell_i^*(-\alpha_i)}{m|\Omega_i|} - \frac{w_j x_{ij}}{m} \right)$ 
9:       end for
10:      send  $\mathbf{w}^{(\sigma_r(q))}$  to machine  $\sigma_{r+1}^{-1}(\sigma_r(q))$  and receive  $\mathbf{w}^{(\sigma_{r+1}(q))}$ 
11:    end for
12:  end for
13:   $t \leftarrow t + 1$ 
14: until convergence

```

3.1 Convergence Proof

We prove finite time convergence of our algorithm with $O(1/\sqrt{T})$ rates.

Theorem 1. Suppose, Algorithm 1 is run with $p \leq \min(m, d)$ processors, and let (\mathbf{w}^t, α^t) and $(\tilde{\mathbf{w}}^t, \tilde{\alpha}^t) := \left(\frac{1}{t} \sum_{s=1}^t \mathbf{w}^s, \frac{1}{t} \sum_{s=1}^t \alpha^s \right)$ denote the parameter values, and the averaged parameter values respectively after the t -th epoch. Moreover, assume that

- There exists a partitioning of Ω such that $|\Omega^{(q, \sigma_r(q))}| \approx \frac{1}{p^2} |\Omega|$ and $|J_q| \approx \frac{d}{p}$ for all q .
- Performing updates (8) takes constant amount of time denoted by T_u .
- Communicating \mathbf{w} across the network takes constant amount of time denoted by T_c , and communicating a subset of \mathbf{w} takes time proportional to its cardinality.
- The diameter of the search space is bounded. In other words, there exists a constant D such that for all (\mathbf{w}, α) and (\mathbf{w}', α') we have $\|\mathbf{w} - \mathbf{w}'\|^2 + \|\alpha - \alpha'\|^2 \leq D$.
- The gradients of $f_{i,j}(w_j, \alpha_i)$ are bounded by a constant that does not depend on i or j .

$$\|\nabla_{\mathbf{w}} f_{i,j}(w_j, \alpha_i)\|^2 \leq C_w^2 \text{ and } \|\nabla_{\alpha} f_{i,j}(w_j, \alpha_i)\|^2 \leq C_{\alpha}^2. \quad (9)$$

Then, there exists a constant C such that after $\left(\frac{|\Omega|T_u}{p} + T_c \right) T$ time, the duality gap is

$$\varepsilon(\mathbf{w}, \alpha) := \max_{\alpha'} f(\tilde{\mathbf{w}}^T, \alpha') - \min_{\mathbf{w}'} f(\mathbf{w}', \tilde{\alpha}^T) \leq \sqrt{\frac{2DC}{T}}. \quad (10)$$

The proof is in Appendix A. The main technical difficulty in proving convergence is that general stochastic analysis cannot be applied directly to DSO; because of its distributed nature DSO does not sample (i, j) coordinates uniformly at random. Therefore, we first show that the updates of DSO are serializable, and then analyze the convergence of this incremental gradient algorithm. The cost we pay for this is a $|\Omega|$ term which is implicit in our problem dependent constant C . In contrast, the rates of Nemirovski et al. [14], who assume uniform sampling, do not contain a dependence on either m , d or $|\Omega|$. Another important note is regarding scalability. Our analysis implies that we need computational time proportional to $O\left(\frac{|\Omega|T_u}{p} + T_c\right)$ to get solution of a certain fixed quality (as measured by the duality gap). This implies that DSO scales linearly in p as long as $\frac{|\Omega|T_u}{p} \gg T_c$ holds. As is to be expected, for large enough p the cost of communication T_c will eventually dominate.

4 Related Work

Effective parallelization of stochastic optimization for regularized risk minimization has received significant research attention in recent years. Because of space limitations, our review of related work will unfortunately only be partial.

The key difficulty in parallelizing update (4) is that gradient calculation requires us to *read*, while updating the parameter requires us to *write* to the coordinates of \mathbf{w} . Consequently, updates have to be executed in serial. Existing work has focused on working around the limitation of stochastic optimization by either a) introducing strategies for computing the stochastic gradient in parallel (e.g., [9]), b) updating the parameter in parallel (e.g., [16]), c) performing independent updates and combining the resulting parameter vectors (e.g., [22]), or d) periodically exchanging information between processors (e.g., Bertsekas and Tsitsiklis [1]). While the former two strategies are popular in the shared memory setting, the latter two are popular in the distributed memory setting. However, in many cases the convergence bounds depend on the amount of correlation between data points. In contrast our bounds in Theorem 1 do not depend on correlations between data points.

Algorithms that use a so-called parameter server to synchronize variable updates across processors have recently become popular (e.g., [12, 18]). The main drawback of these methods is that it is not easy to “serialize” the updates, that is, to replay the updates on a single machine. This makes proving convergence guarantees, and debugging such frameworks rather difficult.

The observation that updates on individual coordinates of the parameters can be carried out in parallel has been used for other models. In the context of Latent Dirichlet Allocation Yan et al. [20] used a similar observation to derive an efficient GPU based collapsed Gibbs sampler. On the other hand, for matrix factorization Gemulla et al. [7] and Recht and Ré [15] independently proposed parallel algorithms based on a similar idea. However, to the best of our knowledge, rewriting (1) as a saddle point problem in order to discover parallelism is our novel contribution.

5 Empirical Evaluation

We conducted single machine experiments with relatively small datasets to verify that stochastic optimization of the saddle point formulation in (6) is a viable strategy for regularized risk minimization. The multi-machine experiments are mainly designed to study convergence behavior. In both settings we work with linear SVM and logistic regression with square norm regularization. Details of the datasets used and additional plots can be found in the supplementary material. Our code and experiment scripts can be downloaded from <http://anonymous>.

We compare DSO against Stochastic Gradient Descent (SGD) and Bundle Methods for Regularized risk Minimization (BMRM) [19]. AdaGrad [5] step size adaptation is used in both SGD and DSO, while BMRM uses the toolkit for advanced optimization (TAO) (<https://bitbucket.org/sarich/tao-2.2>). In multi machine experiments, BMRM is straightforward to parallelize since it is a batch learning algorithm. To parallelize SGD, we used PSGD of Zinkevich et al. [22].

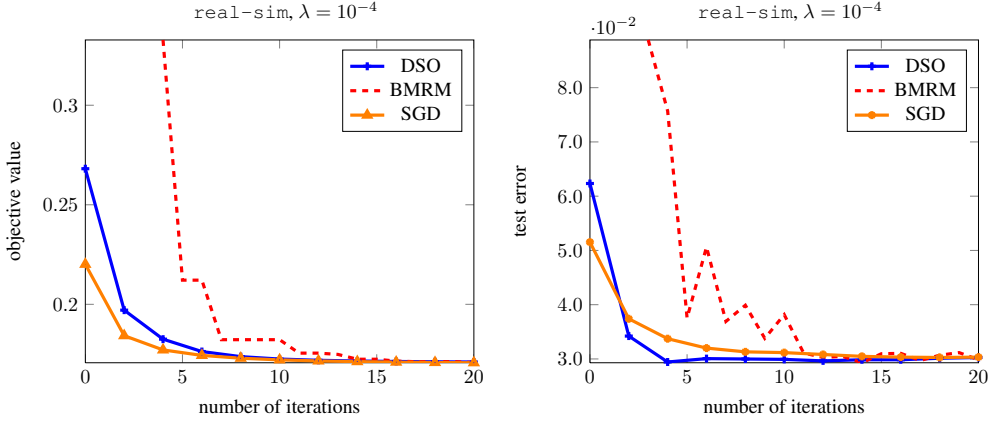


Figure 2: Convergence behavior for SVM on `real-sim` dataset.

5.1 Single Machine Experiments

Due to space constraints, complete results and plots can be found in the supplementary material. In the main body we only present results on the `real-sim` dataset with SVM in Figure 2. As can be seen, DSO is slower than SGD but faster than BMRM. This is to be expected because DSO performs stochastic optimization and is therefore able to beat BMRM which performs batch optimization. However, since DSO optimizes $m + d$ parameters as opposed to d parameters for SGD, we find that DSO is slower than SGD. A similar trend is observed on many other datasets (see supplementary).

5.2 Multi Machine Experiments

In Figure 3, we contrast the convergence behavior of DSO with BMRM and PSGD on `kdda` dataset. As can be seen, DSO converges much faster than BMRM and PSGD both in terms of the number of iterations as well as the actual time spent. On the `ocr` dataset, however, the situation is different (see Figure 4). While DSO is still competitive in terms of the number of iterations, BMRM outperforms in terms of the actual time spent. This is due to the fact that `ocr` is a dense dataset, and hence BMRM is able to make use of optimized numerical linear algebra libraries such as BLAS [10] to streamline memory access and computation. In contrast, DSO which is a stochastic algorithm performs random memory access and consequently is slower. Due to redundancy in the dataset, PSGD outperforms both BMRM and DSO. See supplementary material for results on other datasets.

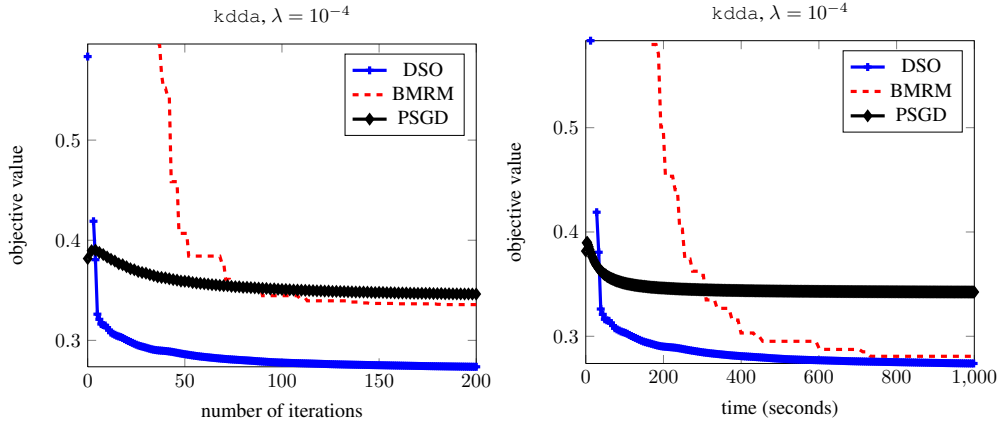


Figure 3: Convergence behavior of SVM on `kdda` (4 machines, 8 cores/machine).

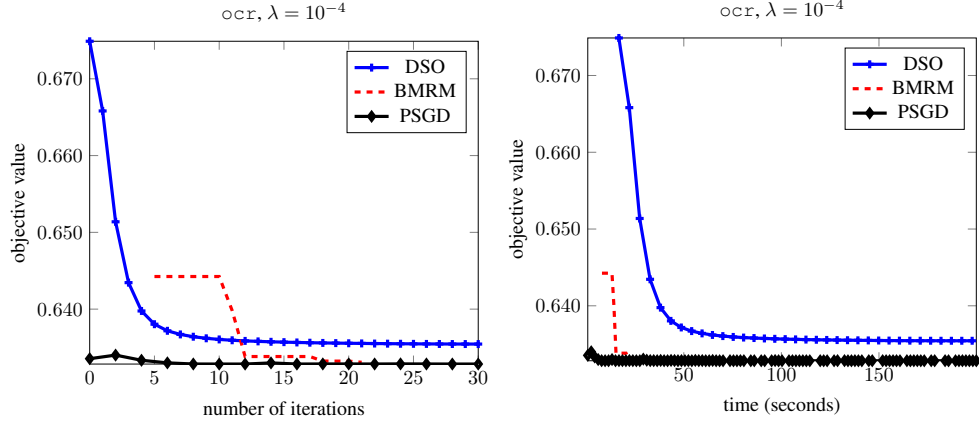


Figure 4: Convergence behavior of SVM on `ocr` (4 machines, 8 cores/machine).

5.3 Scaling of the Algorithm

In this experiment, we vary the number of machines between 1, 2, 4, 8 while fixing the number of cores utilized in each machine to be 8 to study the scaling behavior of DSO. Figure 5 shows the result on `kdda` and `ocr` datasets by plotting the objective value as a function of the number of seconds elapsed \times the number of machines used (Figure 78 in the supplementary material plots the elapsed seconds vs. objective value). If DSO scales linearly, then all lines in the figure should overlap with each other. In `kdda` dataset (left), some slowdown is observed due to very low density of data (1.82e-4%). Between each inner iteration, each machine has to send and receive $\mathbf{w}^{(q)}$ which is of size d/p , so when d is large it requires significant effort. When the data is very sparse, however, there are small number of coordinates to actually process within each inner iteration. On the other hand, on `ocr` dataset (right) the scaling is very nice since it is a dense dataset. It even shows super-linear scaling, thanks to cache locality effects; because the size of the parameter stored in each machine gets smaller as we use larger number of machines, the probability of cache miss gets lower, similar to what happens in the matrix completion problem [21].

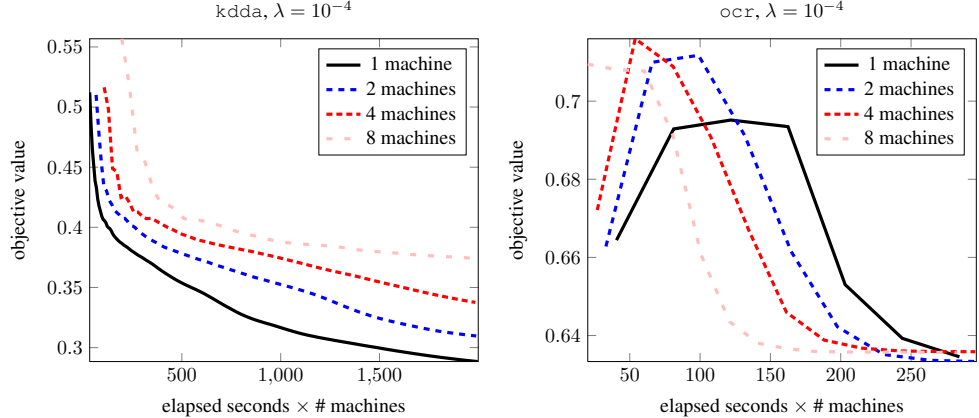


Figure 5: Convergence behavior of SVM on `ocr` with different number of machines.

6 Discussion and Conclusion

We presented a new equivalent formulation of regularized risk minimization as a saddle point problem, and showed that one can derive an efficient distributed stochastic optimizer (DSO). We also proved rates of convergence of DSO. Unlike BMRM, our algorithm does not require any strong

convexity or L_2 Regularization and thus has wider applicability. Our experimental results show that DSO is competitive with batch optimization schemes and comprehensively outperforms stochastic optimization schemes which simply average their parameters after every iteration.

A natural next step is to derive an asynchronous algorithm along the lines of the NOMAD algorithm proposed by Yun et al. [21]. We believe that our convergence proof which only relies on having an equivalent serial sequence of updates will still apply. Of course, there is also significantly more scope to further improve the performance of DSO by deriving better step size adaptation schedules or by exploiting characteristics of specific datasets.

References

- [1] D. Bertsekas and J. Tsitsiklis. *Parallel and Distributed Computation: Numerical Methods*. 1997.
- [2] L. Bottou and O. Bousquet. The tradeoffs of large-scale learning. *Optimization for Machine Learning*, 2011.
- [3] S. Boyd and L. Vandenberghe. *Convex Optimization*. 2004.
- [4] C.-T. Chu, S. K. Kim, Y.-A. Lin, Y. Yu, G. Bradski, A. Y. Ng, and K. Olukotun. Map-reduce for machine learning on multicore. In *NIPS*, pages 281–288, 2006.
- [5] J. Duchi, E. Hazan, and Y. Singer. Adaptive subgradient methods for online learning and stochastic optimization. *Journal of Machine Learning Research*, 12:2121–2159, 2010.
- [6] R.-E. Fan, J.-W. Chang, C.-J. Hsieh, X.-R. Wang, and C.-J. Lin. LIBLINEAR: A library for large linear classification. *Journal of Machine Learning Research*, 9:1871–1874, Aug. 2008.
- [7] R. Gemulla, E. Nijkamp, P. J. Haas, and Y. Sismanis. Large-scale matrix factorization with distributed stochastic gradient descent. In *KDD*, pages 69–77, 2011.
- [8] T. Hastie, R. Tibshirani, and J. Friedman. *The Elements of Statistical Learning*. 2009.
- [9] J. Langford, A. J. Smola, and M. Zinkevich. Slow learners are fast. In *NIPS*, 2009.
- [10] C. L. Lawson, R. J. Hanson, D. Kincaid, and F. T. Krogh. Basic linear algebra subprograms for FORTRAN usage. *ACM Transactions on Mathematical Software*, 5:308–323, 1979.
- [11] D. C. Liu and J. Nocedal. On the limited memory BFGS method for large scale optimization. *Mathematical Programming*, 45(3):503–528, 1989.
- [12] Y. Low, J. Gonzalez, A. Kyrola, D. Bickson, C. Guestrin, and J. M. Hellerstein. Distributed graphlab: A framework for machine learning and data mining in the cloud. In *VLDB*, 2012.
- [13] A. Nedić and D. P. Bertsekas. Incremental subgradient methods for nondifferentiable optimization. *SIAM Journal on Optimization*, 12(1):109–138, 2001.
- [14] A. Nemirovski, A. Juditsky, G. Lan, and A. Shapiro. Robust stochastic approximation approach to stochastic programming. *SIAM J. on Optimization*, 19(4):1574–1609, Jan. 2009.
- [15] B. Recht and C. Ré. Parallel stochastic gradient algorithms for large-scale matrix completion. *Mathematical Programming Computation*, 5(2):201–226, June 2013.
- [16] B. Recht, C. Re, S. Wright, and F. Niu. Hogwild: A lock-free approach to parallelizing stochastic gradient descent. In *NIPS*, pages 693–701, 2011.
- [17] B. Schölkopf and A. J. Smola. *Learning with Kernels*. 2002.
- [18] A. J. Smola and S. Narayanamurthy. An architecture for parallel topic models. In *VLDB*, 2010.
- [19] C. H. Teo, S. V. N. Vishwanathan, A. J. Smola, and Q. V. Le. Bundle methods for regularized risk minimization. *Journal of Machine Learning Research*, 11:311–365, January 2010.
- [20] F. Yan, N. Xu, and Y. Qi. Parallel inference for latent Dirichlet allocation on graphics processing units. In *NIPS*, pages 2134–2142. 2009.
- [21] H. Yun, H.-F. Yu, C.-J. Hsieh, S. V. N. Vishwanathan, and I. S. Dhillon. Nomad: Non-locking, stochastic multi-machine algorithm for asynchronous and decentralized matrix completion. *CoRR*, abs/1312.0193, 2013.
- [22] M. Zinkevich, A. J. Smola, M. Weimer, and L. Li. Parallelized stochastic gradient descent. In *NIPS*, pages 2595–2603, 2010.

A Proof of Theorem 1

The proof consists of two steps. First we prove that DSO is serializable in a certain sense, that is, there exists an ordering of the updates such that *replaying* them on a single machine recovers the solution produced by DSO. Next, we use somewhat standard convergence results (e.g., [13]) to establish convergence of this serial algorithm.

Let (\mathbf{w}^t, α^t) denote the parameter vector after the t -th epoch. Without loss of generality, we will focus on the inner iterations of the $(t+1)$ -st epoch. Consider a time instance at which k updates corresponding to $(i_1, j_1), (i_2, j_2), \dots, (i_k, j_k)$ have been performed on (\mathbf{w}^t, α^t) , which results in the parameter values denoted by $(\mathbf{w}_k^t, \alpha_k^t)$. There is a natural ordering of updates as follows: (i_a, j_a) appears before (i_b, j_b) if updates to (w_{j_a}, α_{i_a}) were performed before updating (w_{j_b}, α_{i_b}) . On the other hand, if (w_{j_a}, α_{i_a}) and (w_{j_b}, α_{i_b}) were updated at the same time because we have p processors simultaneously updating the parameters, then the updates are ordered according to the rank of the processor performing the update. The following lemma asserts that the updates are serializable in the sense that $(\mathbf{w}_k^t, \alpha_k^t)$ can be recovered by performing k serial updates on function f_k which is defined below.

Lemma 2. *For all k and t we have*

$$\mathbf{w}_k^t = \mathbf{w}_{k-1}^t - \eta_t \nabla_{\mathbf{w}} f_k(\mathbf{w}_{k-1}^t, \alpha_{k-1}^t) \text{ and} \quad (11)$$

$$\alpha_k^t = \alpha_{k-1}^t - \eta_t \nabla_{\alpha} f_k(\mathbf{w}_{k-1}^t, \alpha_{k-1}^t), \quad (12)$$

where

$$f_k(\mathbf{w}, \alpha) := f_{i_k, j_k}(w_{j_k}, \alpha_{i_k}).$$

Proof. Let q be the processor which performed the k -th update in the $(t+1)$ -st epoch. Moreover, let $(k-\delta)$ be the most recent previous update done by processor q . There exists $\delta \geq \delta', \delta'' \geq 1$ such that $(\mathbf{w}_{k-\delta'}^t, \alpha_{k-\delta''}^t)$ be the parameter values read by the q -th processor to the perform k -th update. Because of our data partitioning scheme, only q can change the value of the i_k -th component of α and the j_k -th component of \mathbf{w} . Therefore, we have

$$\alpha_{k-1, i_k}^t = \alpha_{\kappa, i_k}^t \quad k - \delta \leq \kappa \leq k - 1 \quad (13)$$

$$w_{k-1, j_k} = w_{\kappa, j_k}^t \quad k - \delta \leq \kappa \leq k - 1 \quad (14)$$

Since f_k is invariant to changes in any coordinate other than (i_k, j_k) , we have

$$f_k(\mathbf{w}_{k-\delta'}^t, \alpha_{k-\delta''}^t) = f_k(\mathbf{w}_{k-1}^t, \alpha_{k-1}^t). \quad (15)$$

The claim holds because we can write the k -th update formula as

$$\mathbf{w}_k^t = \mathbf{w}_{k-1}^t - \eta_t \nabla_{\mathbf{w}} f_k(\mathbf{w}_{k-\delta'}^t, \alpha_{k-\delta''}^t) \text{ and} \quad (16)$$

$$\alpha_k^t = \alpha_{k-1}^t - \eta_t \nabla_{\alpha} f_k(\mathbf{w}_{k-\delta'}^t, \alpha_{k-\delta''}^t). \quad (17)$$

□

As a consequence of the above lemma, it suffices to analyze the serial convergence of the function $f(\mathbf{w}, \alpha) := \sum_k f_k(\mathbf{w}, \alpha)$. Towards this end, we first prove the following technical lemma.

Lemma 3. *Suppose there exists constants C and D such that for all (\mathbf{w}, α) and (\mathbf{w}', α') we have $\|\mathbf{w} - \mathbf{w}'\|^2 + \|\alpha - \alpha'\|^2 \leq D$, and for all $t = 1, \dots, T$ and all (\mathbf{w}, α) we have*

$$\|\mathbf{w}^{t+1} - \mathbf{w}\|^2 + \|\alpha^{t+1} - \alpha\|^2 \leq \|\mathbf{w}^t - \mathbf{w}\|^2 + \|\alpha^t - \alpha\|^2 - 2\eta_t (f(\mathbf{w}^t, \alpha) - f(\mathbf{w}, \alpha^t)) + \eta_t^2 C, \quad (18)$$

then setting $\eta_t = \sqrt{\frac{D}{2Ct}}$ ensures that

$$\varepsilon(\tilde{\mathbf{w}}^T, \tilde{\alpha}^T) \leq \sqrt{\frac{2DC}{T}}. \quad (19)$$

Proof. Rearrange (18) and divide by η_t to obtain

$$2(f(\mathbf{w}^t, \alpha) - f(\mathbf{w}, \alpha^t)) \leq \frac{1}{\eta_t} (\|\mathbf{w}^t - \mathbf{w}\|^2 + \|\alpha^t - \alpha\|^2 - \|\mathbf{w}^{t+1} - \mathbf{w}\|^2 - \|\alpha^{t+1} - \alpha\|^2) + \eta_t C.$$

Summing the above for $t = 1, \dots, T$ yields

$$\begin{aligned} 2 \sum_{t=1}^T f(\mathbf{w}^t, \alpha) - 2 \sum_{t=1}^T f(\mathbf{w}, \alpha^t) &\leq \frac{1}{\eta_1} (\|\mathbf{w}^1 - \mathbf{w}\|^2 + \|\alpha^1 - \alpha\|^2) \\ &\quad + \sum_{t=2}^{T-1} \left(\frac{1}{\eta_{t+1}} - \frac{1}{\eta_t} \right) (\|\mathbf{w}^t - \mathbf{w}\|^2 + \|\alpha^t - \alpha\|^2) \\ &\quad - \frac{1}{\eta_T} (\|\mathbf{w}^{T+1} - \mathbf{w}\|^2 + \|\alpha^{T+1} - \alpha\|^2) + \sum_{t=1}^T \eta_t C \\ &\leq \frac{1}{\eta_1} D + \sum_{t=2}^{T-1} \left(\frac{1}{\eta_{t+1}} - \frac{1}{\eta_t} \right) D + \sum_{t=1}^T \eta_t C \\ &\leq \frac{1}{\eta_T} D + \sum_{t=1}^T \eta_t C. \end{aligned} \tag{20}$$

Thanks to convexity

$$f(\bar{\mathbf{w}}^T, \alpha) = f\left(\frac{1}{T} \sum_{t=1}^T \mathbf{w}^t, \alpha\right) \leq \frac{1}{T} \sum_{t=1}^T f(\mathbf{w}^t, \alpha), \text{ and} \tag{21}$$

$$-f(\mathbf{w}, \bar{\alpha}^T) = -f\left(\mathbf{w}, \frac{1}{T} \sum_{t=1}^T \alpha^t\right) \leq \frac{1}{T} \sum_{t=1}^T -f(\mathbf{w}, \alpha^t). \tag{22}$$

Substituting (21) and (22) into (20), and letting $\eta_t = \sqrt{\frac{D}{2Ct}}$ leads to the following sequence of inequalities

$$f(\bar{\mathbf{w}}^T, \alpha) - f(\mathbf{w}, \bar{\alpha}^T) \leq \frac{\frac{1}{\eta_T} D + \sum_{t=1}^T \eta_t C}{2T} \leq \sqrt{\frac{DC}{2T}} + \frac{\sqrt{DC}}{2T} \sum_{t=1}^T \frac{1}{\sqrt{2t}}.$$

The claim in (19) follows by using $\sum_{t=1}^T \frac{1}{\sqrt{2t}} \leq \sqrt{2T}$. \square

To prove convergence of DSO it suffices to show that it satisfies (18). The proof closely follows techniques outlined in e [13].

Lemma 4. *Under the assumptions outlined in Theorem 1, Algorithm 1 satisfies (18).*

Proof.

$$\begin{aligned} \|\mathbf{w}_k^t - \mathbf{w}\|^2 &= \|\mathbf{w}_{k-1}^t - \eta_t \nabla_{\mathbf{w}} f_k(\mathbf{w}_{k-1}^t, \alpha_{k-1}^t) - \mathbf{w}\|^2 \\ &= \|\mathbf{w}_{k-1}^t - \mathbf{w}\|^2 - 2\eta_t \langle \nabla_{\mathbf{w}} f_k(\mathbf{w}_{k-1}^t, \alpha_{k-1}^t), \mathbf{w}_{k-1}^t - \mathbf{w} \rangle + \eta_t^2 \|\nabla_{\mathbf{w}} f_k(\mathbf{w}_{k-1}^t, \alpha_{k-1}^t)\|^2 \\ &\leq \|\mathbf{w}_{k-1}^t - \mathbf{w}\|^2 - 2\eta_t \langle \nabla_{\mathbf{w}} f_k(\mathbf{w}_{k-1}^t, \alpha_{k-1}^t), \mathbf{w}_{k-1}^t - \mathbf{w} \rangle + \eta_t^2 C_w^2 \\ &\leq \|\mathbf{w}_{k-1}^t - \mathbf{w}\|^2 - 2\eta_t (f_k(\mathbf{w}_{k-1}^t, \alpha_{k-1}^t) - f_k(\mathbf{w}, \alpha_{k-1}^t)) + \eta_t^2 C_w^2 \end{aligned}$$

Analogously for α we have

$$\|\alpha_k^t - \alpha\|^2 \leq \|\alpha_{k-1}^t - \alpha\|^2 - 2\eta_t (-f_k(\mathbf{w}_{k-1}^t, \alpha_{k-1}^t) + f_k(\mathbf{w}_{k-1}^t, \alpha)) + \eta_t^2 C_\alpha^2$$

Adding the above two inequalities, rearranging

$$\begin{aligned} \|\mathbf{w}_k^t - \mathbf{w}\|^2 + \|\alpha_k^t - \alpha\|^2 - \|\mathbf{w}_{k-1}^t - \mathbf{w}\|^2 - \|\alpha_{k-1}^t - \alpha\|^2 &\leq -2\eta_t (f_k(\mathbf{w}_{k-1}^t, \alpha) - f_k(\mathbf{w}, \alpha_{k-1}^t)) \\ &\quad + \eta_t^2 (C_w^2 + C_\alpha^2), \end{aligned}$$

and summing the above equation for $k = 1, \dots, |\Omega|$ obtains

$$\begin{aligned}
& \|\mathbf{w}^{t+1} - \mathbf{w}\|^2 + \|\boldsymbol{\alpha}^{t+1} - \boldsymbol{\alpha}\|^2 - \|\mathbf{w}^t - \mathbf{w}\|^2 - \|\boldsymbol{\alpha}^t - \boldsymbol{\alpha}\|^2 \\
& \leq -2\eta_t \left(\sum_k f_k(\mathbf{w}_{k-1}^t, \boldsymbol{\alpha}) - f_k(\mathbf{w}^t, \boldsymbol{\alpha}) + \sum_k -f_k(\mathbf{w}, \boldsymbol{\alpha}_{k-1}^t) - (-f_k(\mathbf{w}, \boldsymbol{\alpha}^t)) \right) \\
& \quad - 2\eta_t (f(\mathbf{w}^t, \boldsymbol{\alpha}) - f(\mathbf{w}, \boldsymbol{\alpha}^t)) + \eta_t^2 \sum_k (C_w^2 + C_\alpha^2). \tag{23}
\end{aligned}$$

Next observe that

$$\begin{aligned}
f_k(\mathbf{w}^t, \boldsymbol{\alpha}) - f_k(\mathbf{w}_{k-1}^t, \boldsymbol{\alpha}) & \leq \langle \mathbf{w}_{k-1}^t - \mathbf{w}^t, \nabla_{\mathbf{w}} f_k(\mathbf{w}^t, \boldsymbol{\alpha}) \rangle \\
& \leq \|\mathbf{w}_{k-1}^t - \mathbf{w}^t\| \|\nabla_{\mathbf{w}} f_k(\mathbf{w}^t, \boldsymbol{\alpha})\| \\
& \leq \left\| \sum_{j=1}^{k-1} \eta_t \nabla_{\mathbf{w}} f_k(\mathbf{w}_{j-1}^t, \boldsymbol{\alpha}) \right\| \|\nabla_{\mathbf{w}} f_k(\mathbf{w}^t, \boldsymbol{\alpha})\| \\
& \leq \eta_t \sum_{j=1}^{k-1} C_w^2 = \eta_t (k-1) C_w^2.
\end{aligned}$$

and similarly

$$-f_k(\mathbf{w}, \boldsymbol{\alpha}_{k-1}^t) - (-f_k(\mathbf{w}, \boldsymbol{\alpha}^t)) \leq \eta_t (k-1) C_\alpha^2.$$

Incorporating this bound into (23), we get

$$\begin{aligned}
& \|\mathbf{w}^{t+1} - \mathbf{w}\|^2 + \|\boldsymbol{\alpha}^{t+1} - \boldsymbol{\alpha}\|^2 - \|\mathbf{w}^t - \mathbf{w}\|^2 - \|\boldsymbol{\alpha}^t - \boldsymbol{\alpha}\|^2 \\
& \leq 2\eta_t \left(\eta_t C_w^2 \sum_k (k-1) + \eta_t C_\alpha^2 \sum_k (k-1) \right) - 2\eta_t (f(\mathbf{w}^t, \boldsymbol{\alpha}) - f(\mathbf{w}, \boldsymbol{\alpha}^t)) + \eta_t^2 \sum_k (C_w^2 + C_\alpha^2) \\
& = -2\eta_t (f(\mathbf{w}^t, \boldsymbol{\alpha}) - f(\mathbf{w}, \boldsymbol{\alpha}^t)) + \eta_t^2 (C_w^2 + C_\alpha^2) \sum_k (2k-1). \\
& = -2\eta_t (f(\mathbf{w}^t, \boldsymbol{\alpha}) - f(\mathbf{w}, \boldsymbol{\alpha}^t)) + \eta_t^2 (C_w^2 + C_\alpha^2) |\Omega|^2.
\end{aligned}$$

Setting $C = (C_w^2 + C_\alpha^2) |\Omega|^2$ recovers (18). \square

The time complexity bounds follow immediately from the following observation: Processor q pays a computational cost of

$$\left| \Omega^{(q, \sigma_r(q))} \right| T_u + \frac{|J_{\sigma_r(q)}|}{d} T_c \approx \frac{|\Omega| T_u}{p^2} + \frac{T_c}{p},$$

per inner iteration of Algorithm 1. Since there are p inner iterations per epoch, the time consumed by one epoch is $\frac{|\Omega| T_u}{p} + T_c$, and hence the time consumed by T epochs is $\left(\frac{|\Omega| T_u}{p} + T_c \right) T$ as claimed.

B Implementation Details

Our code is implemented in portable C++ and uses the MPICH2 library which provides an implementation of the Message Passing Interface, MPI, for inter-machine communication.

To prevent degeneracy in logistic regression, values of α_i 's are projected to lie in the range $(10^{-14}, 1 - 10^{-14})$, while in the case of linear SVM it is projected to $[0, 1]$. Similarly, the w_j 's are restricted to lie in the interval $[-1/\sqrt{\lambda}, 1/\sqrt{\lambda}]$ for linear SVM and $[-\sqrt{\log(2)/\lambda}, \sqrt{\log(2)/\lambda}]$ for logistic regression. As for step size tuning, we used AdaGrad algorithm of Duchi et al. [5].

In serial experiments, w_j parameters are initialized to be 0; α_i parameters are initialized to be 0 as well in SVM experiments, and 0.0005 in logistic regression experiments. In parallel experiments, each MPI process executed dual coordinate descent [6] on its local data to locally initialize w_j and α_i parameters; then w_j values were averaged across all machines.

Table 2: Summary of the datasets used in our experiments. m is the total # of examples, d is the # of features, s is the feature density (% of features that are non-zero), $m_+ : m_-$ is the ratio of the number of positive vs negative examples, Datasize is the size of the data file on disk. M/G denotes a million/billion.

Name	m	d	$ \Omega $	$s(\%)$	$m_+ : m_-$	Size
reuters-ccat	23149	47236	1.76M	0.161	0.87	0.04GB
real-sim	57763	20958	2.97M	0.245	0.44	0.07 GB
news20	15960	1.36 M	7.26M	0.033	1.00	0.11 GB
worm	0.82M	804	0.17G	25.12	0.06	0.93 GB
alpha	0.4M	500	0.20G	100	0.99	2.74 GB
kdda	8.41M	20.22M	0.31G	1.82e-4	6.56	2.55 GB
kddb	19.26M	29.89M	0.59G	1.02e-4	7.91	4.90 GB
ocr	2.8 M	1156	3.24G	100	0.96	43.18 GB
dna	40 M	800	8.00G	25.0	3e-3	63.04 GB

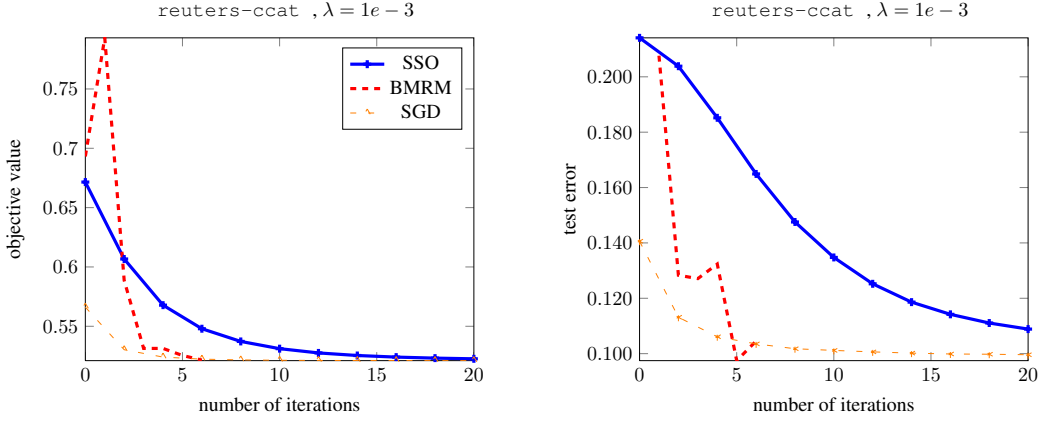


Figure 6: Serial logistic regression experiment on reuters-ccat dataset with regularization parameter $1e-3$

C Dataset Details

D Serial Experiments

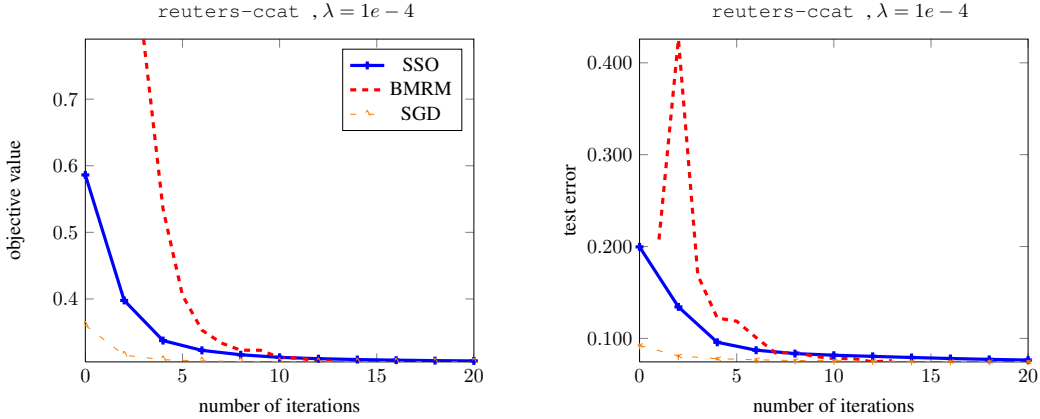


Figure 7: Serial logistic regression experiment on reuters-ccat dataset with regularization parameter $1e-4$

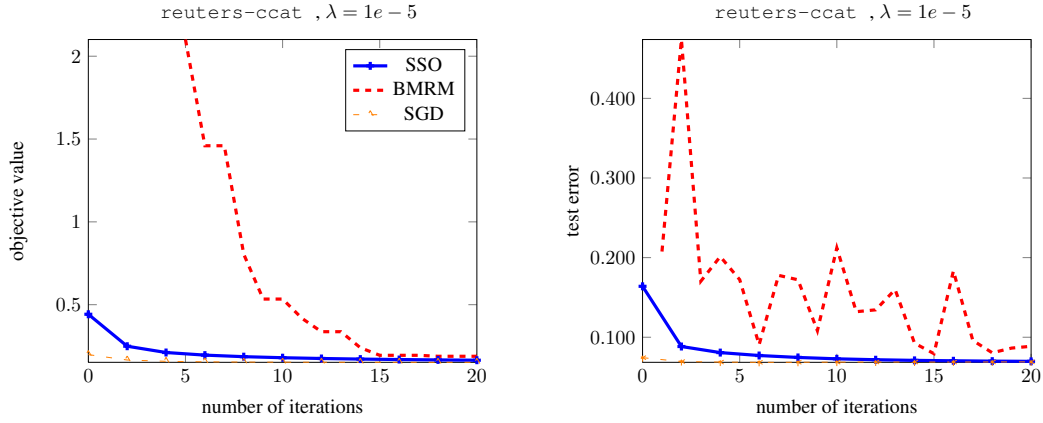


Figure 8: Serial logistic regression experiment on REUTERS-CCAT dataset with regularization parameter $1e-5$

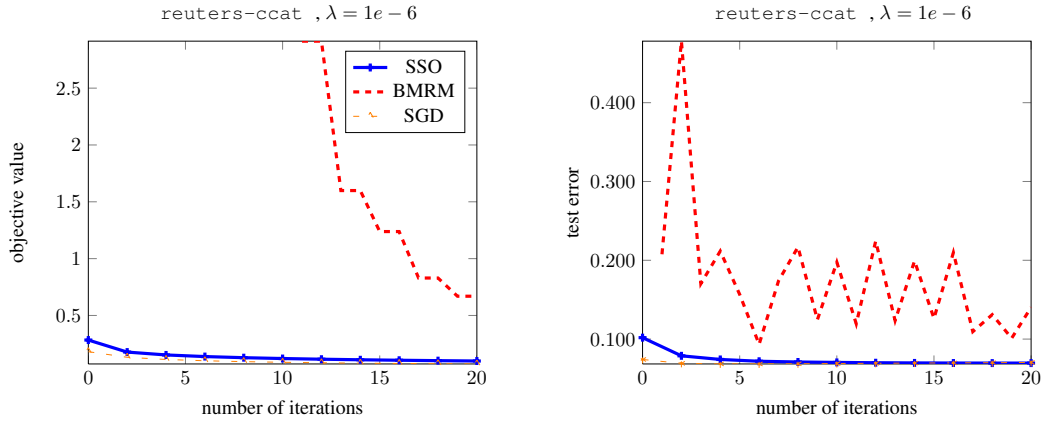


Figure 9: Serial logistic regression experiment on REUTERS-CCAT dataset with regularization parameter $1e-6$

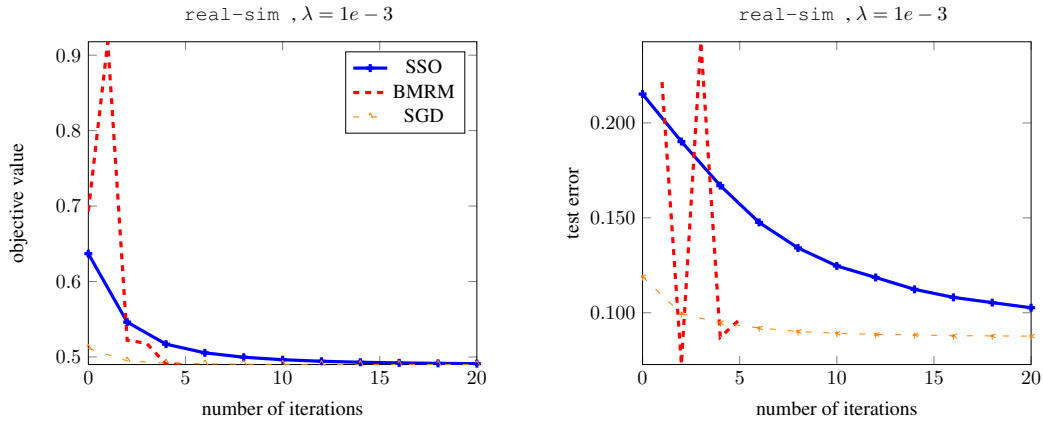


Figure 10: Serial logistic regression experiment on real-sim dataset with regularization parameter $1e-3$

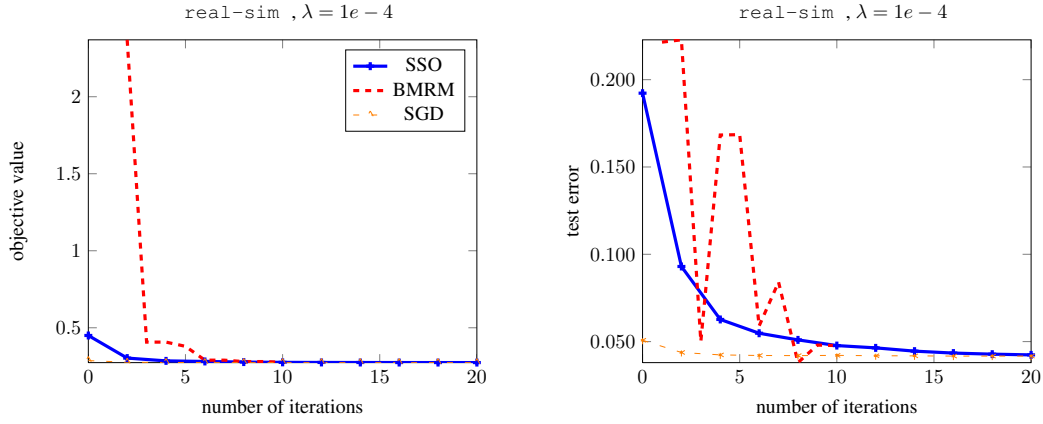


Figure 11: Serial logistic regression experiment on real-sim dataset with regularization parameter $1e-4$

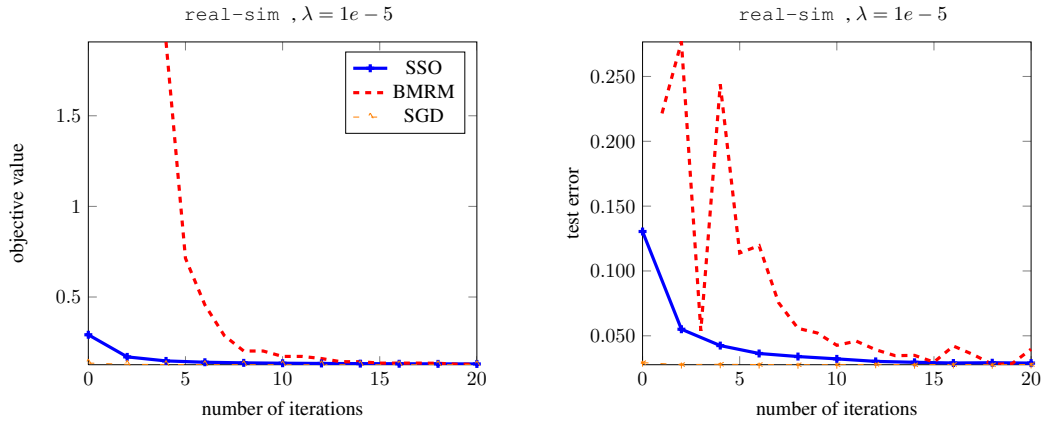


Figure 12: Serial logistic regression experiment on real-sim dataset with regularization parameter $1e-5$

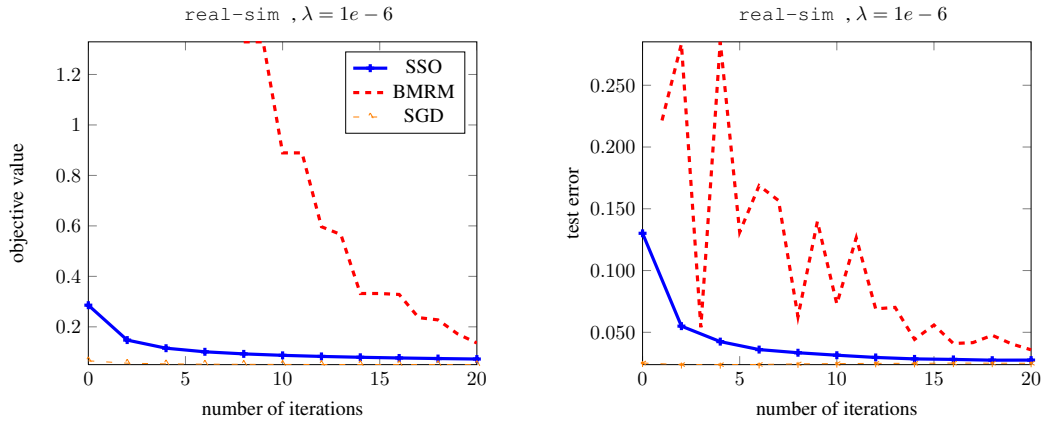


Figure 13: Serial logistic regression experiment on real-sim dataset with regularization parameter $1e-6$

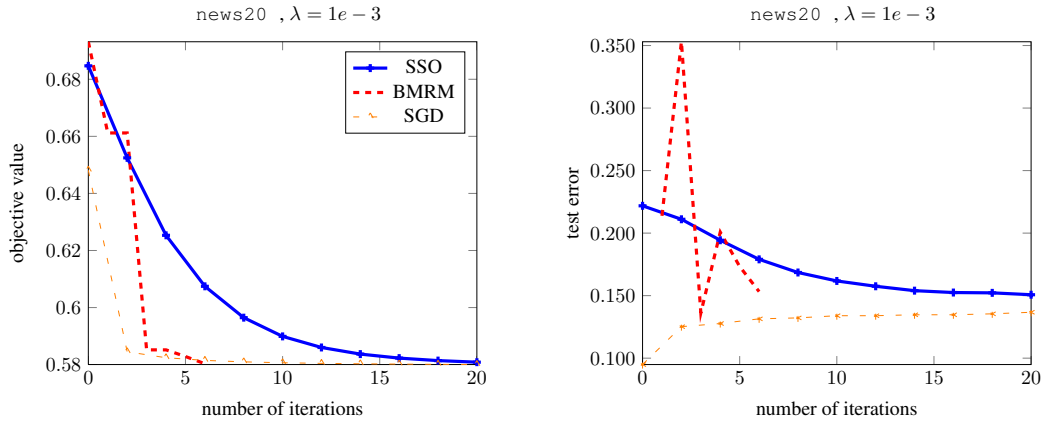


Figure 14: Serial logistic regression experiment on news20 dataset with regularization parameter $1e-3$

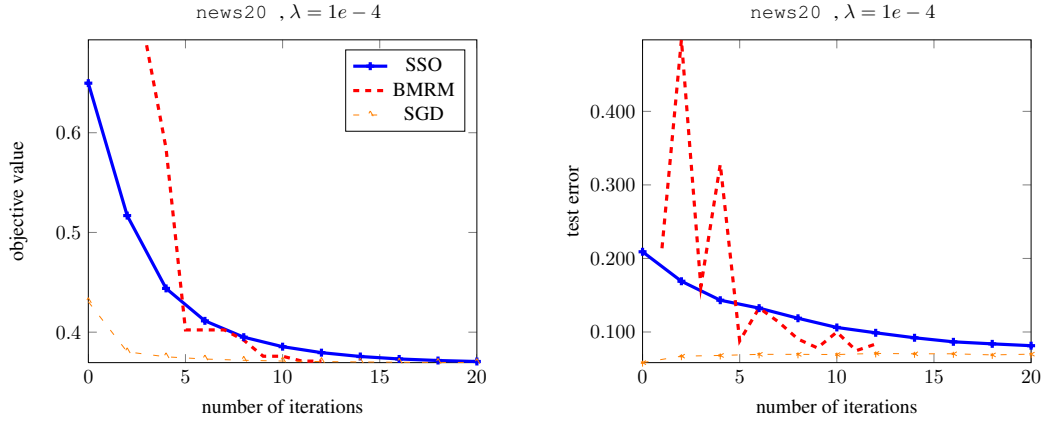


Figure 15: Serial logistic regression experiment on news20 dataset with regularization parameter $1e-4$

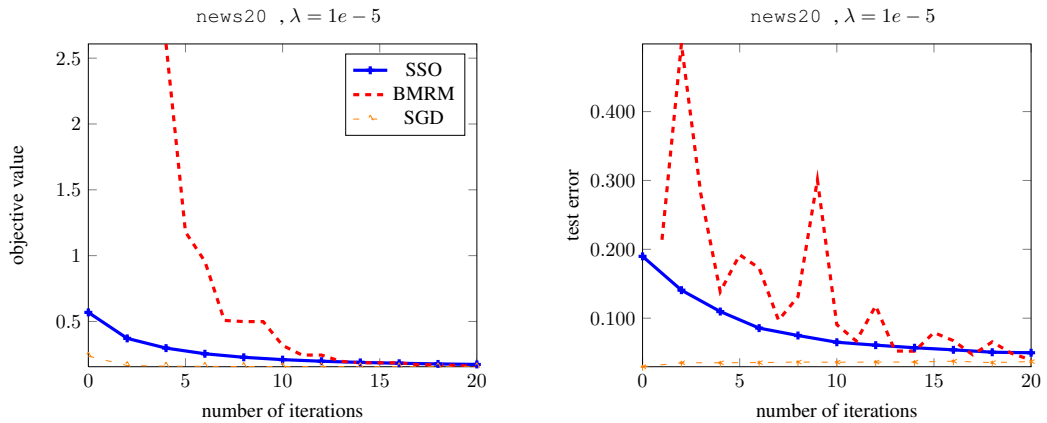


Figure 16: Serial logistic regression experiment on news20 dataset with regularization parameter $1e-5$

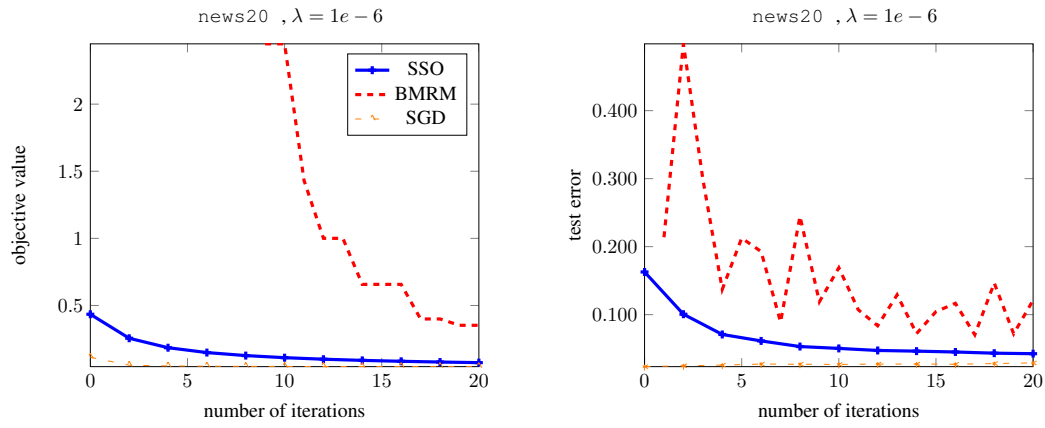


Figure 17: Serial logistic regression experiment on news20 dataset with regularization parameter $1e-6$

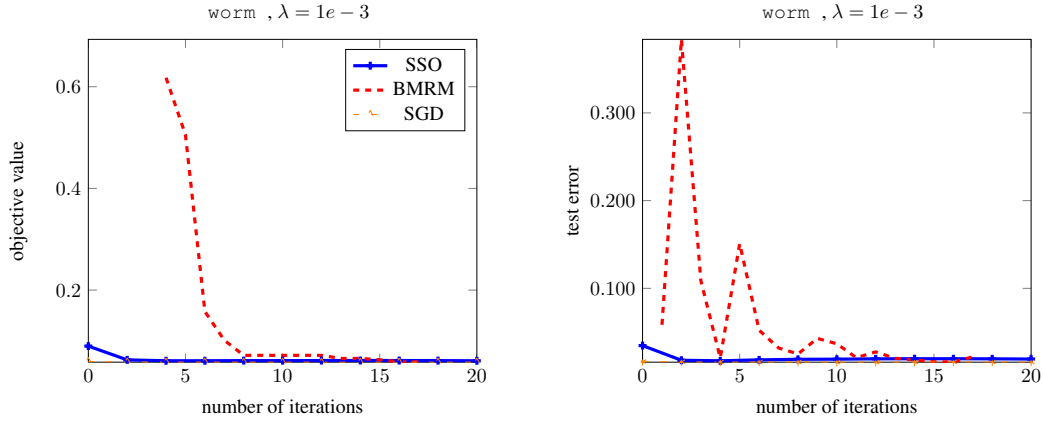


Figure 18: Serial logistic regression experiment on worm dataset with regularization parameter $1e-3$

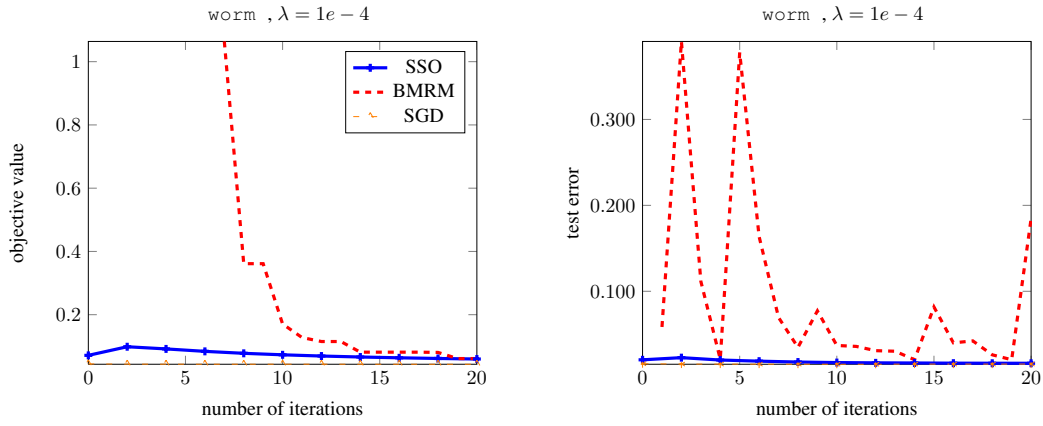


Figure 19: Serial logistic regression experiment on worm dataset with regularization parameter $1e-4$

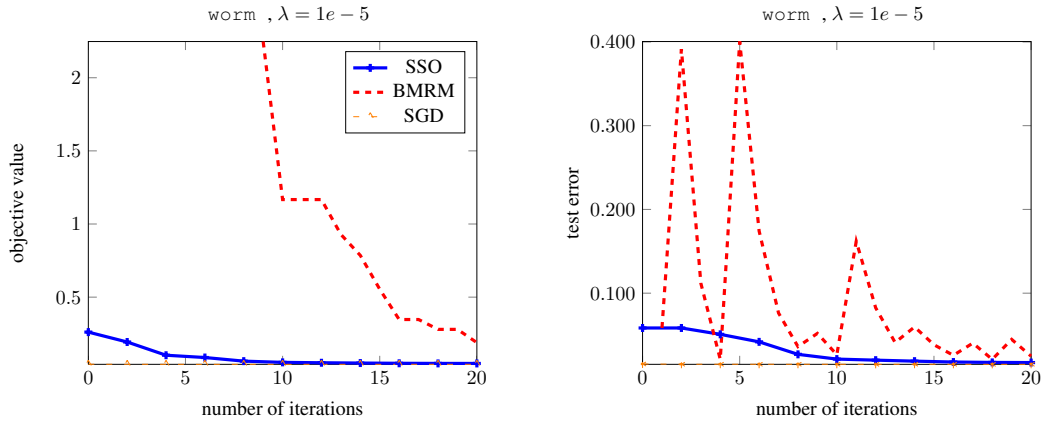


Figure 20: Serial logistic regression experiment on worm dataset with regularization parameter $1e-5$

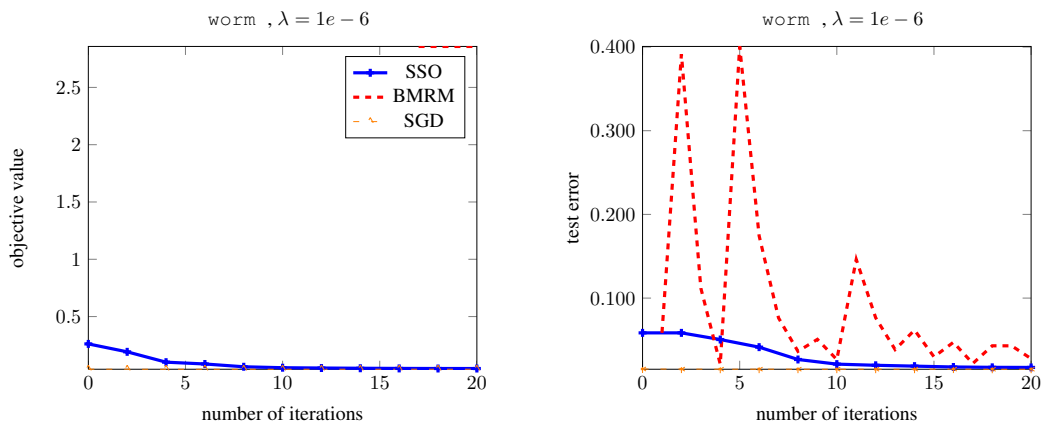


Figure 21: Serial logistic regression experiment on worm dataset with regularization parameter $1e-6$

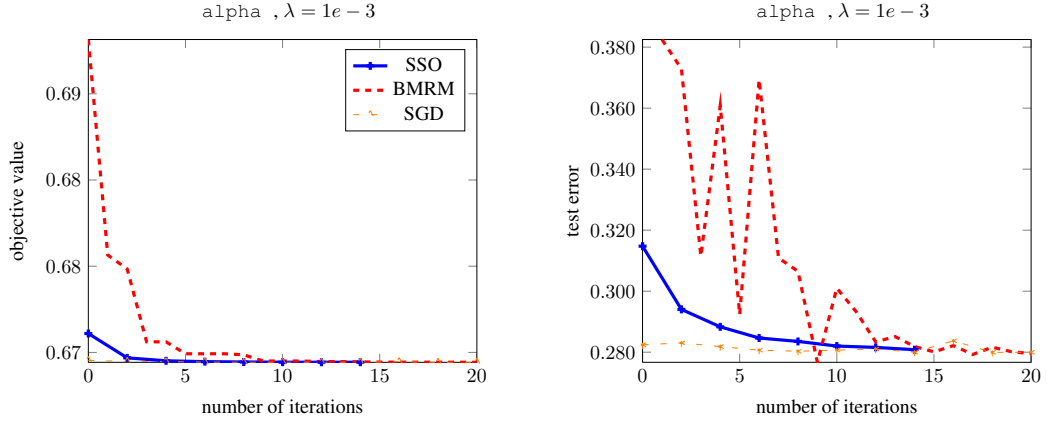


Figure 22: Serial logistic regression experiment on alpha dataset with regularization parameter $1e-3$

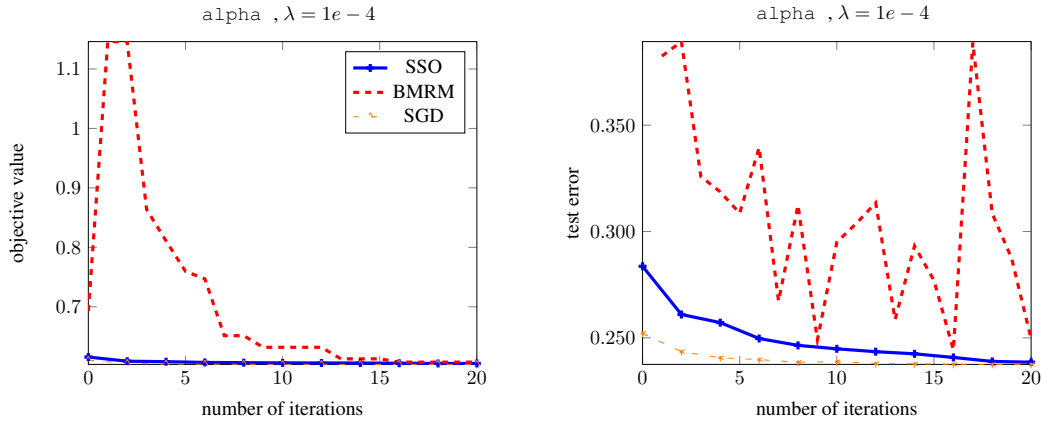


Figure 23: Serial logistic regression experiment on alpha dataset with regularization parameter $1e-4$

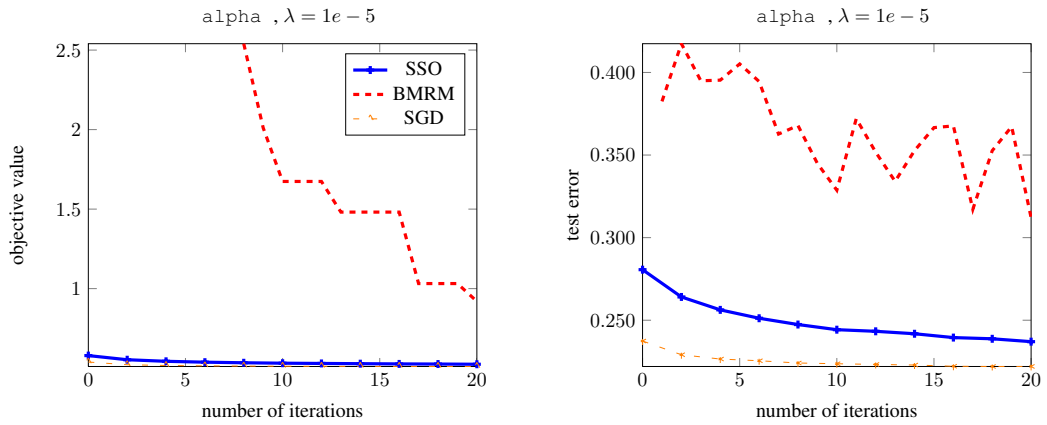


Figure 24: Serial logistic regression experiment on alpha dataset with regularization parameter $1e-5$

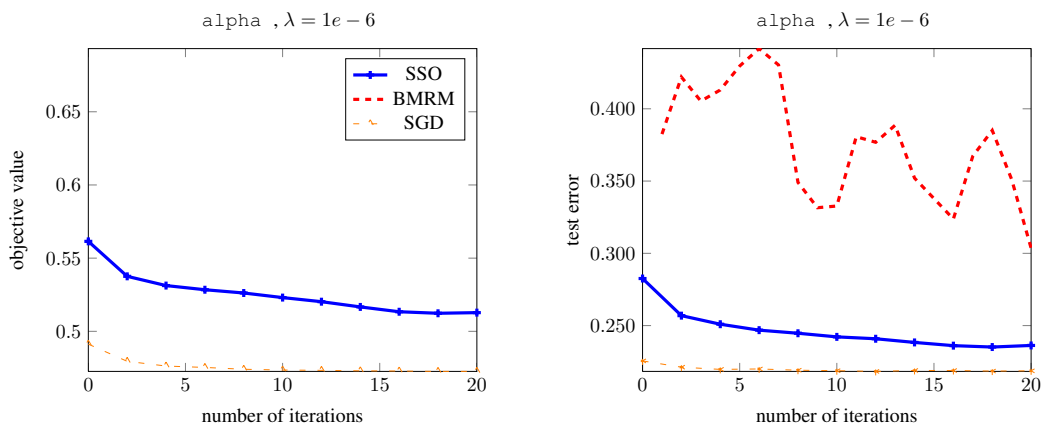


Figure 25: Serial logistic regression experiment on alpha dataset with regularization parameter $1e-6$

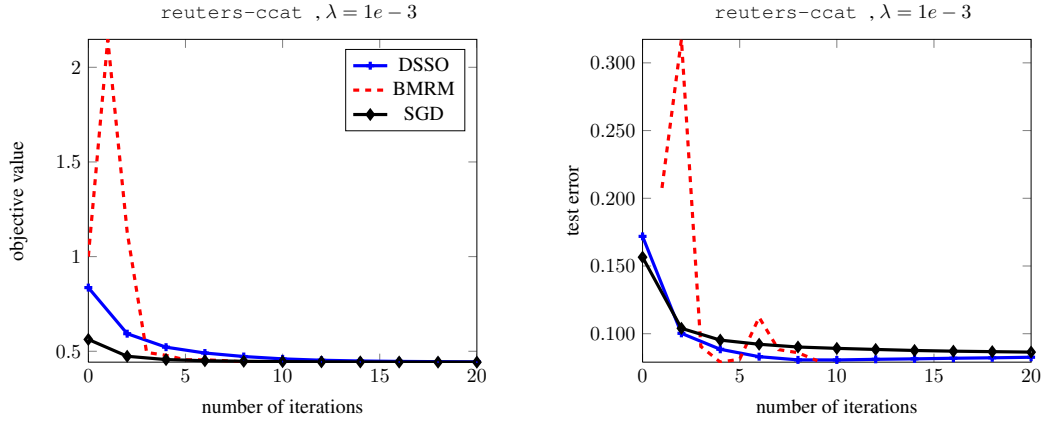


Figure 26: Serial SVM experiment on REUTERS-CCAT dataset with regularization parameter $1e-3$

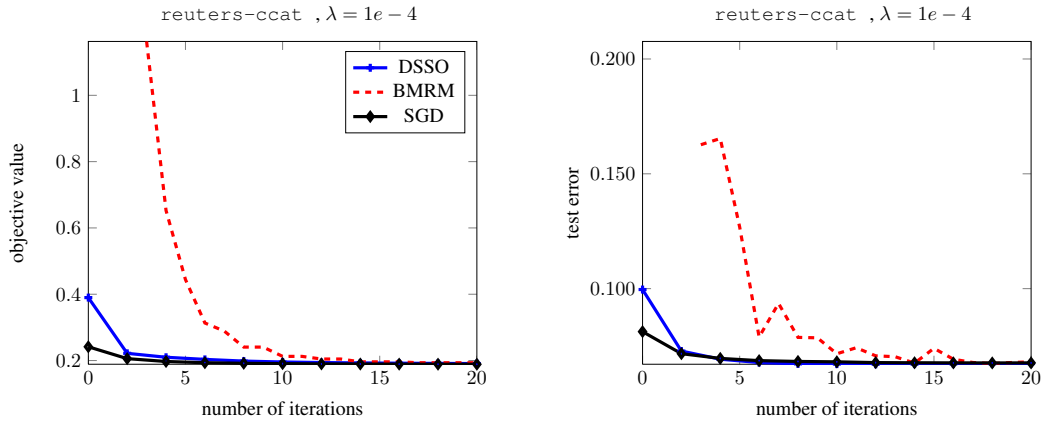


Figure 27: Serial SVM experiment on REUTERS-CCAT dataset with regularization parameter $1e-4$

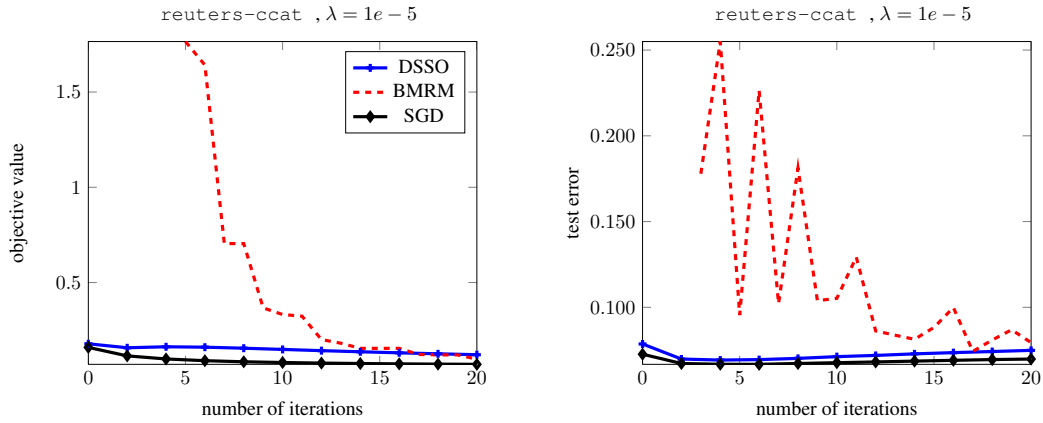


Figure 28: Serial SVM experiment on REUTERS-CCAT dataset with regularization parameter $1e-5$

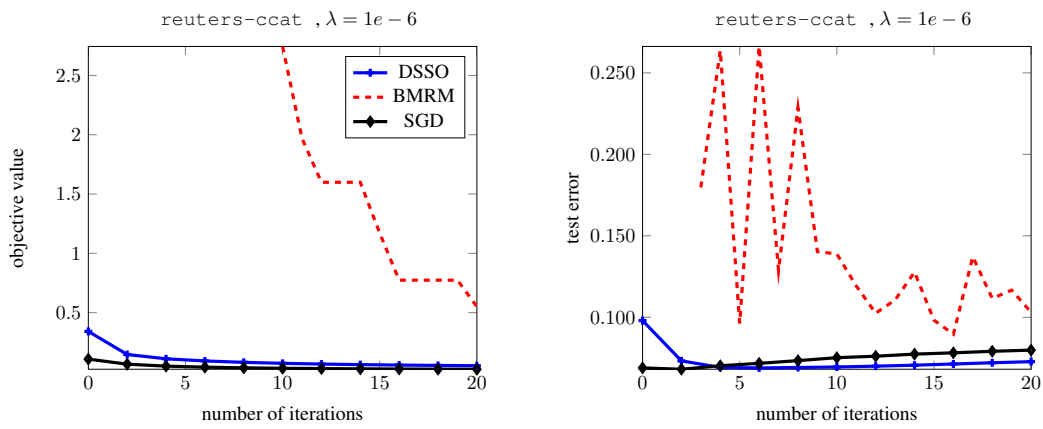


Figure 29: Serial SVM experiment on reuters-ccat dataset with regularization parameter $1e-6$

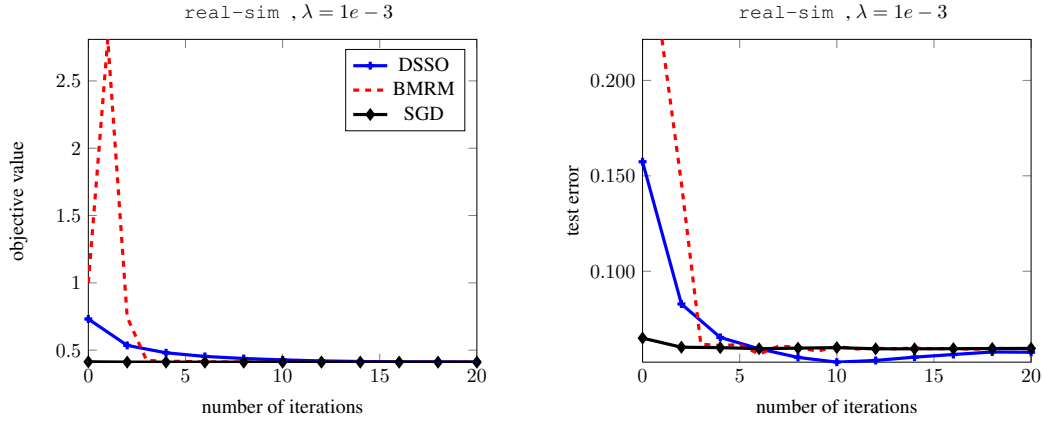


Figure 30: Serial SVM experiment on real-sim dataset with regularization parameter $1e-3$

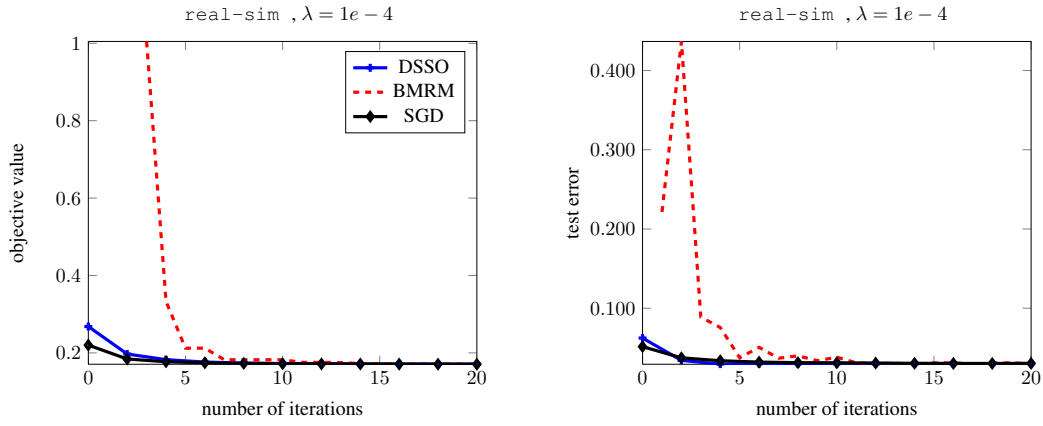


Figure 31: Serial SVM experiment on real-sim dataset with regularization parameter $1e-4$

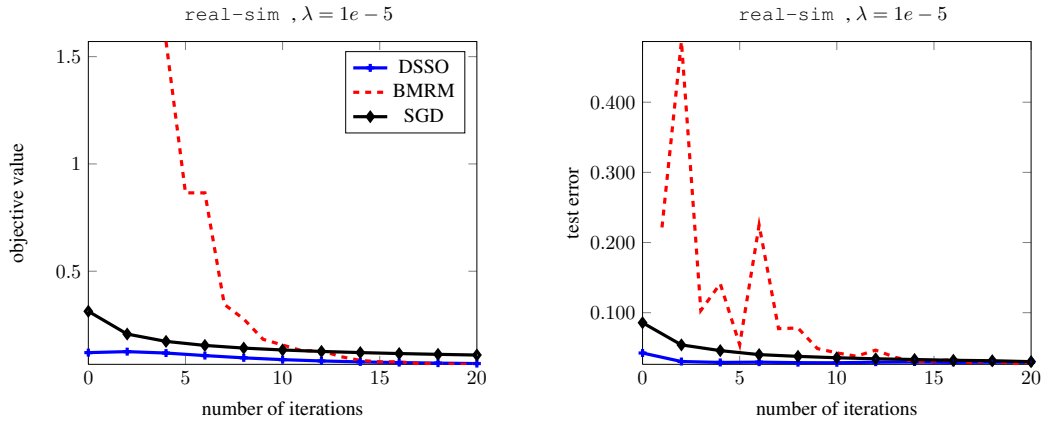


Figure 32: Serial SVM experiment on real-sim dataset with regularization parameter $1e-5$

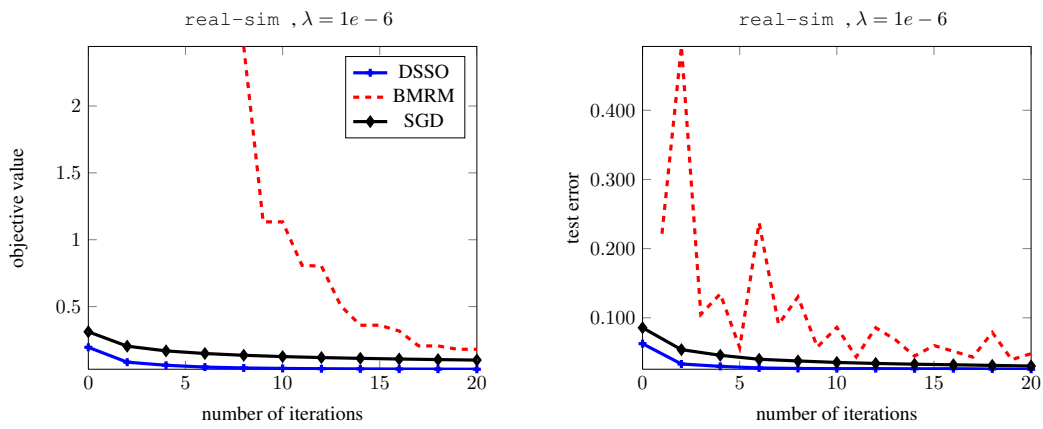


Figure 33: Serial SVM experiment on real-sim dataset with regularization parameter $1e-6$

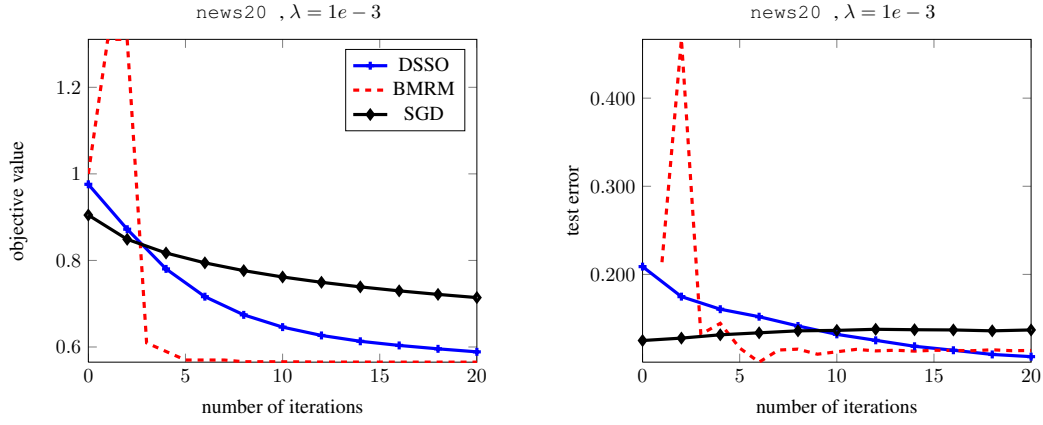


Figure 34: Serial SVM experiment on news20 dataset with regularization parameter $1e-3$

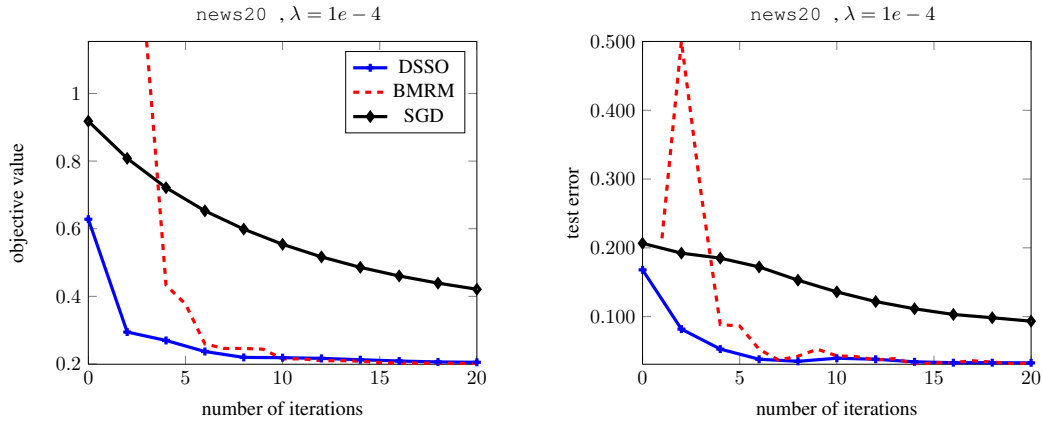


Figure 35: Serial SVM experiment on news20 dataset with regularization parameter $1e-4$

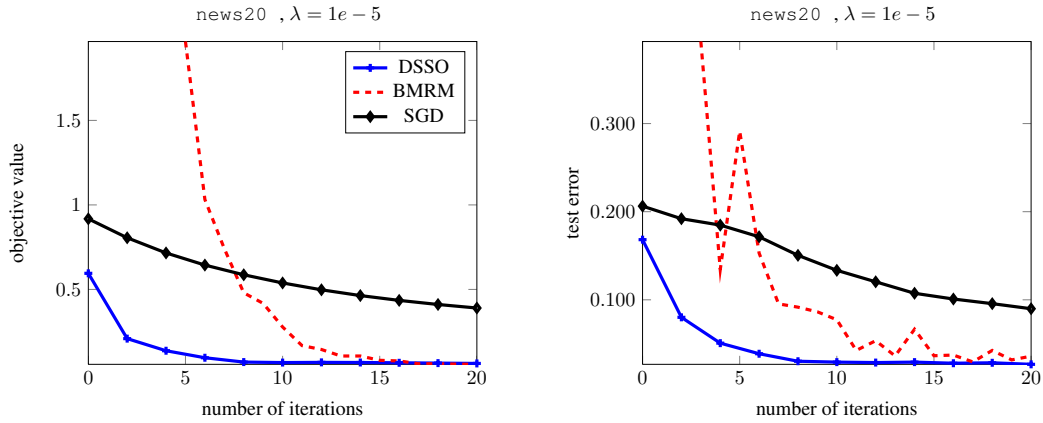


Figure 36: Serial SVM experiment on news20 dataset with regularization parameter $1e-5$

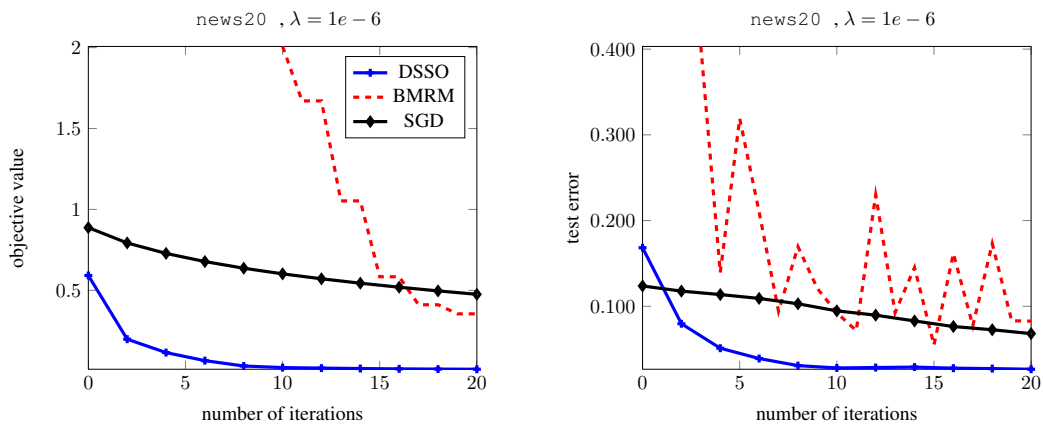


Figure 37: Serial SVM experiment on news20 dataset with regularization parameter $1e-6$

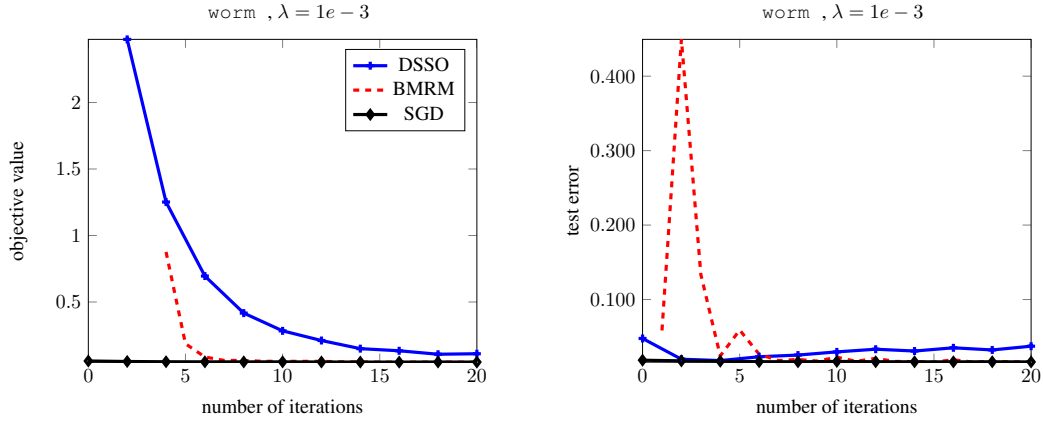


Figure 38: Serial SVM experiment on worm dataset with regularization parameter $1e-3$

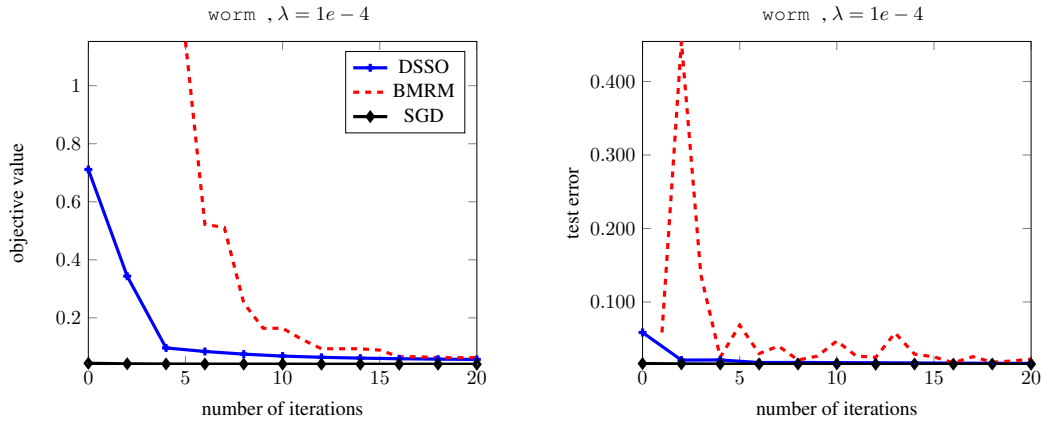


Figure 39: Serial SVM experiment on worm dataset with regularization parameter $1e-4$

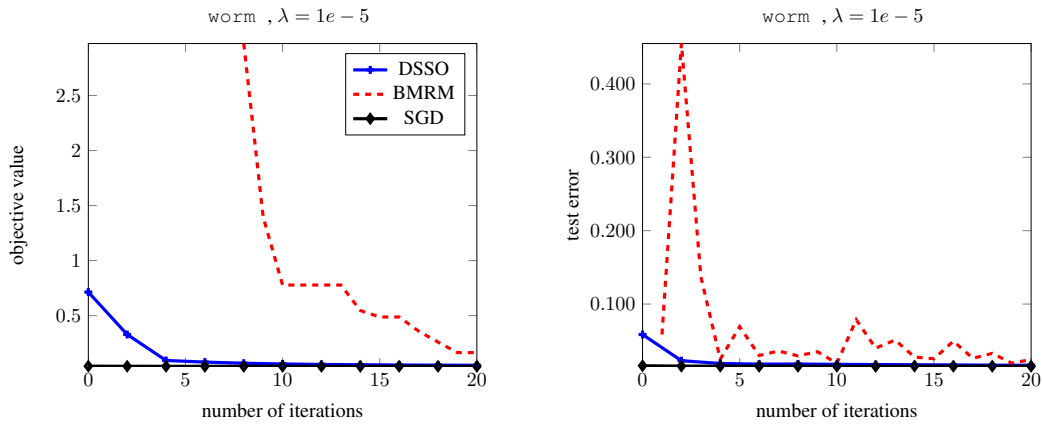


Figure 40: Serial SVM experiment on worm dataset with regularization parameter $1e-5$

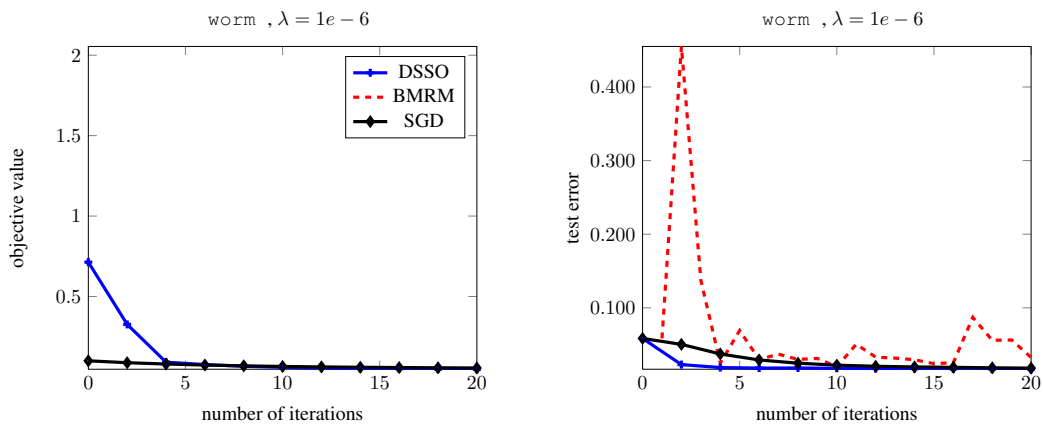


Figure 41: Serial SVM experiment on worm dataset with regularization parameter $1e-6$

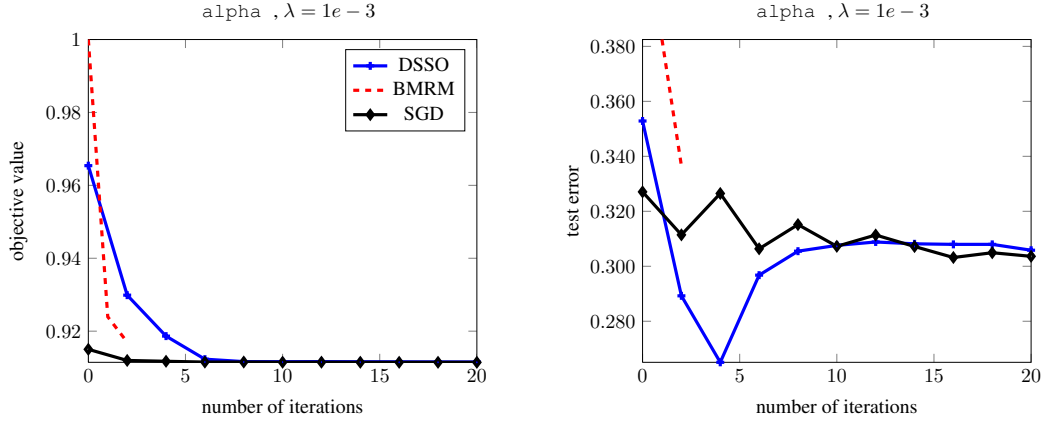


Figure 42: Serial SVM experiment on alpha dataset with regularization parameter $1e-3$

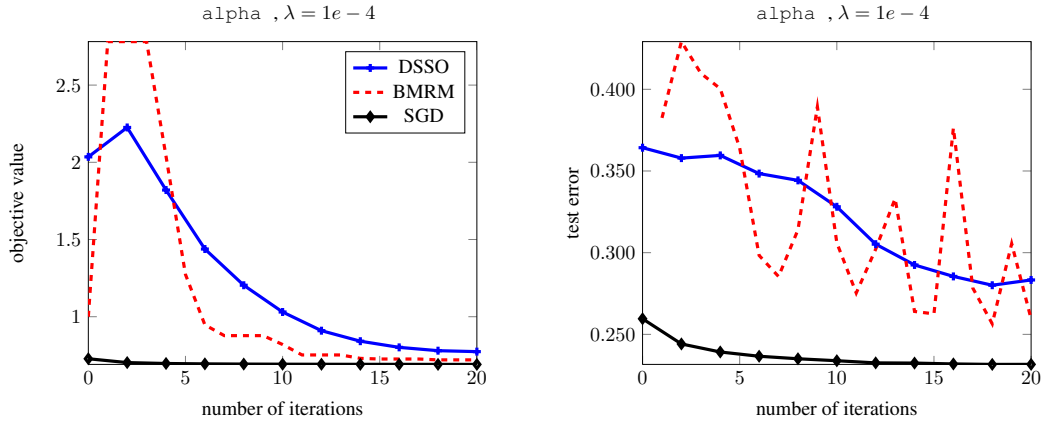


Figure 43: Serial SVM experiment on alpha dataset with regularization parameter $1e-4$

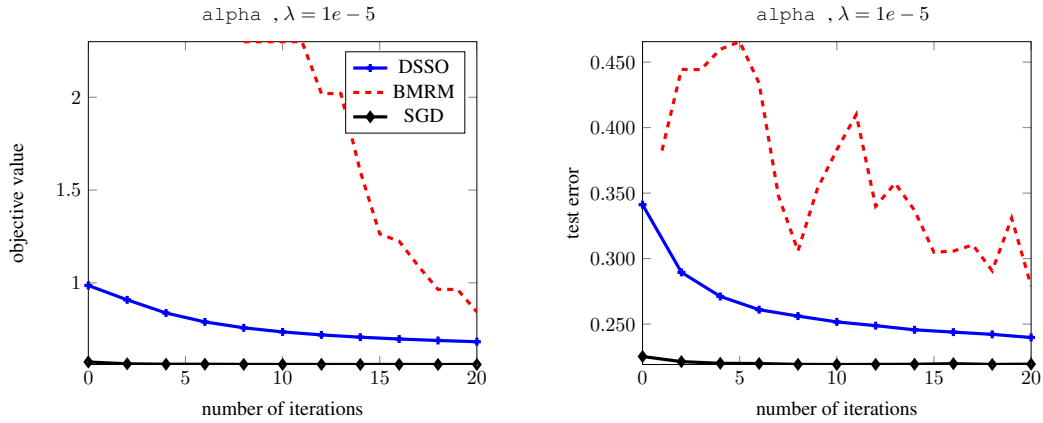


Figure 44: Serial SVM experiment on alpha dataset with regularization parameter $1e-5$

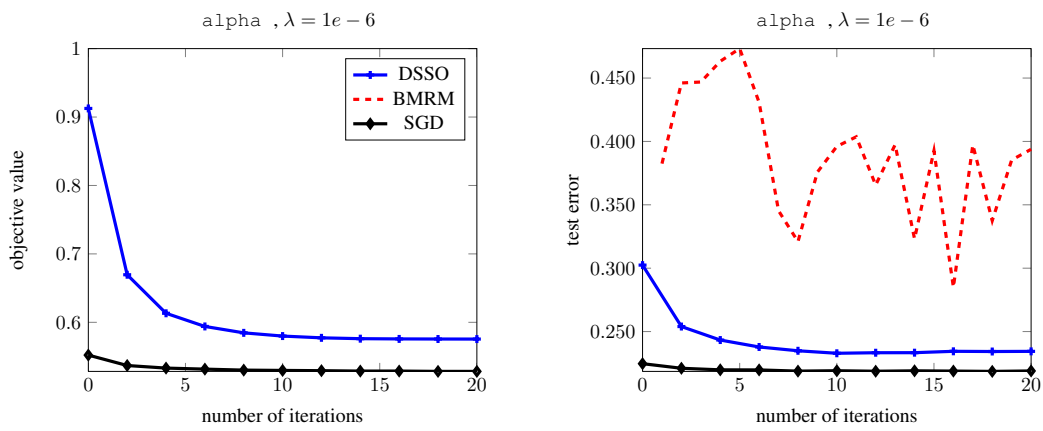


Figure 45: Serial SVM experiment on alpha dataset with regularization parameter $1e-6$

E Parallel Experiments

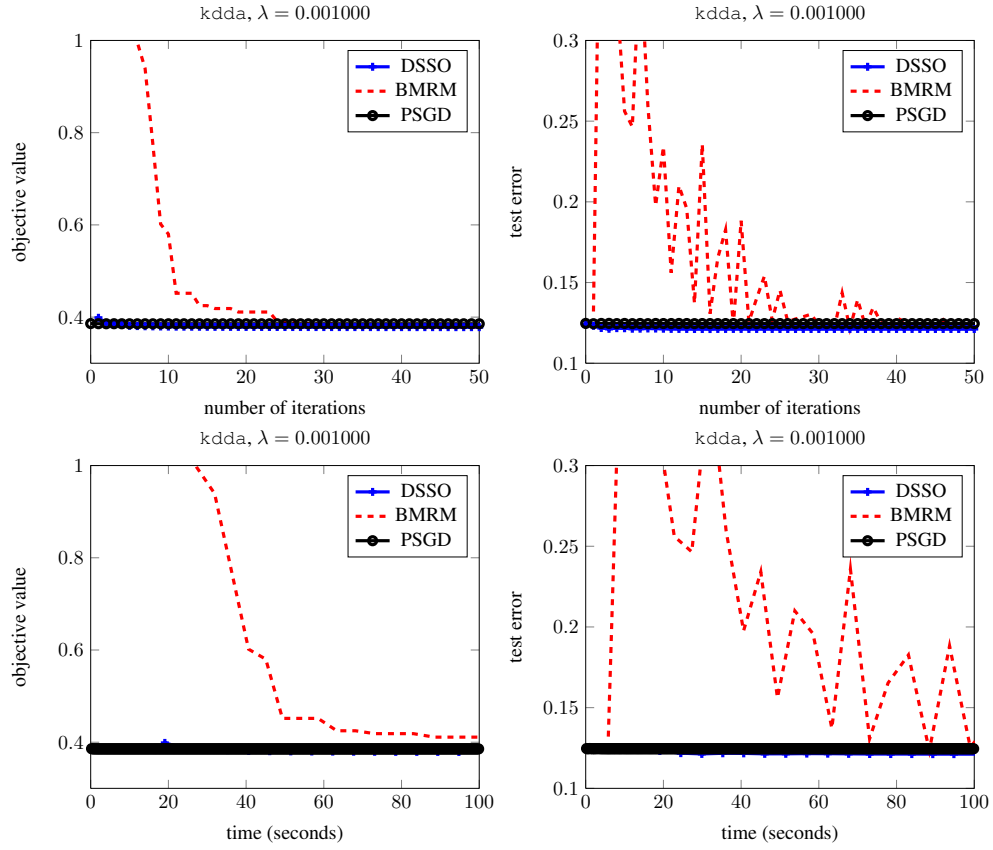


Figure 46: Parallel experiments on kdda dataset with logistic loss. Regularization parameter was set to be 0.001000. We used 4 machines with utilizing 8 cores on each of them. In top figures the x -axis is the number of iterations, while in bottom figures it is the time spent. On the left, the y -axis is the objective value, while on the right it is the test error.

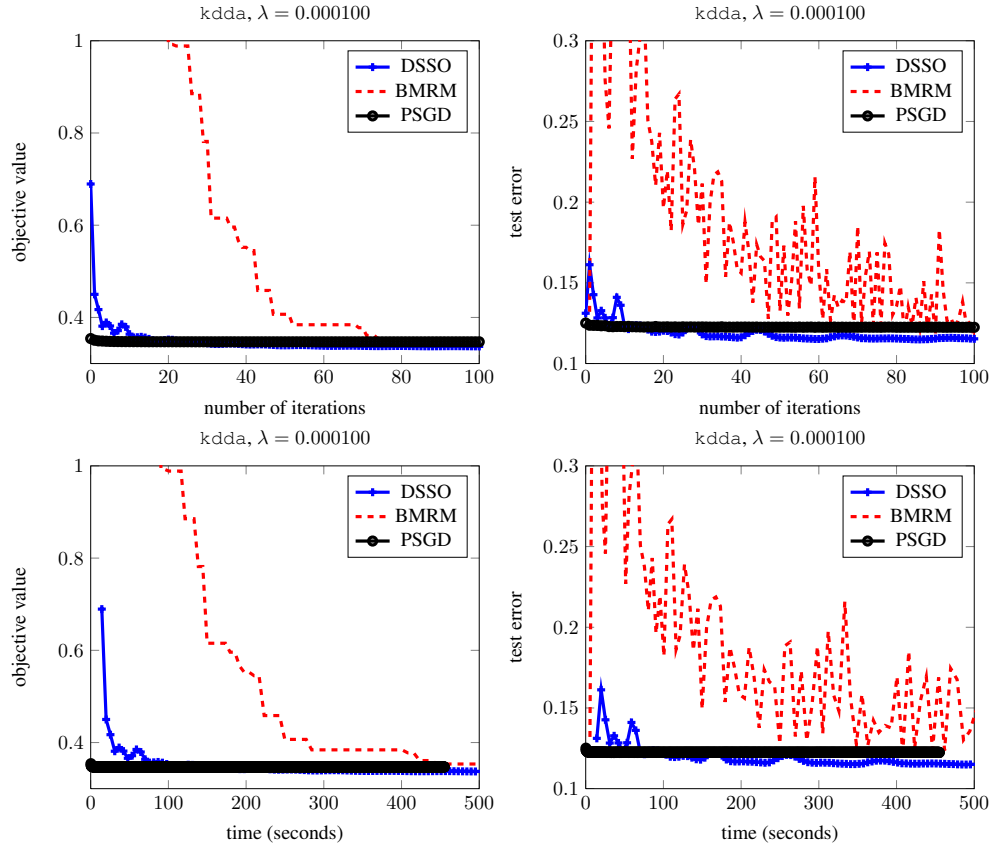


Figure 47: Parallel experiments on kdda dataset with logistic loss. Regularization parameter was set to be 0.000100. We used 4 machines with utilizing 8 cores on each of them. In top figures the x -axis is the number of iterations, while in bottom figures it is the time spent. On the left, the y -axis is the objective value, while on the right it is the test error.

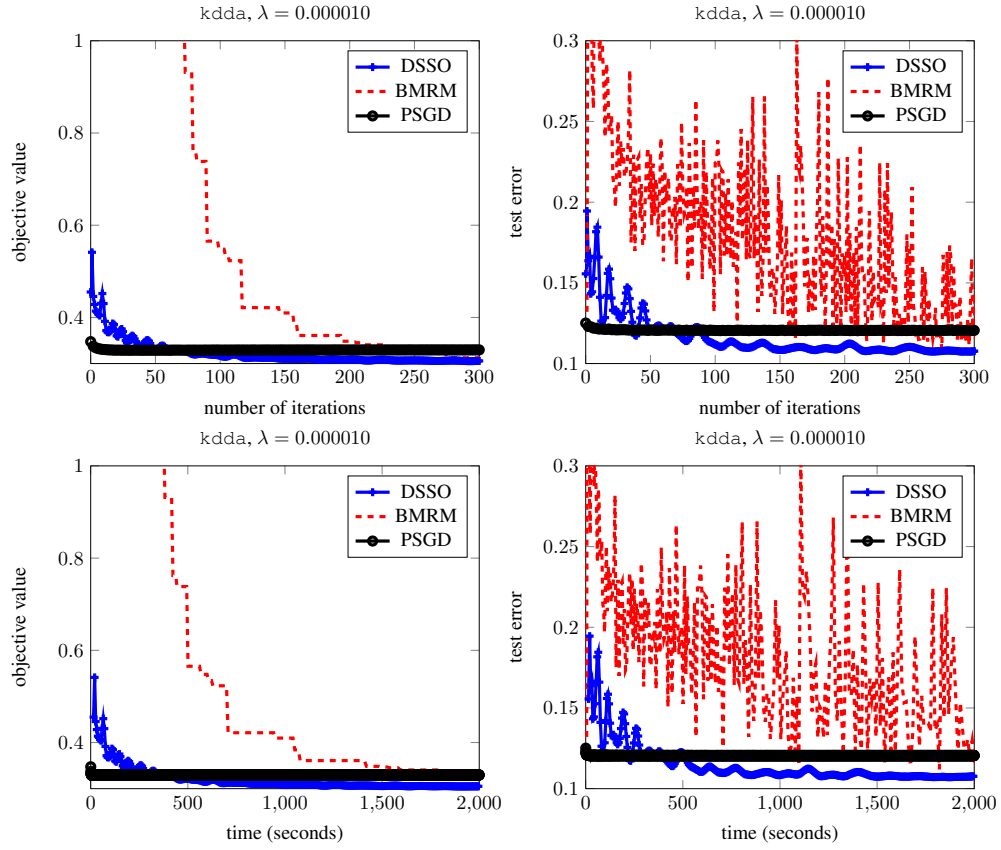


Figure 48: Parallel experiments on kdda dataset with logistic loss. Regularization parameter was set to be 0.000010. We used 4 machines with utilizing 8 cores on each of them. In top figures the x -axis is the number of iterations, while in bottom figures it is the time spent. On the left, the y -axis is the objective value, while on the right it is the test error.

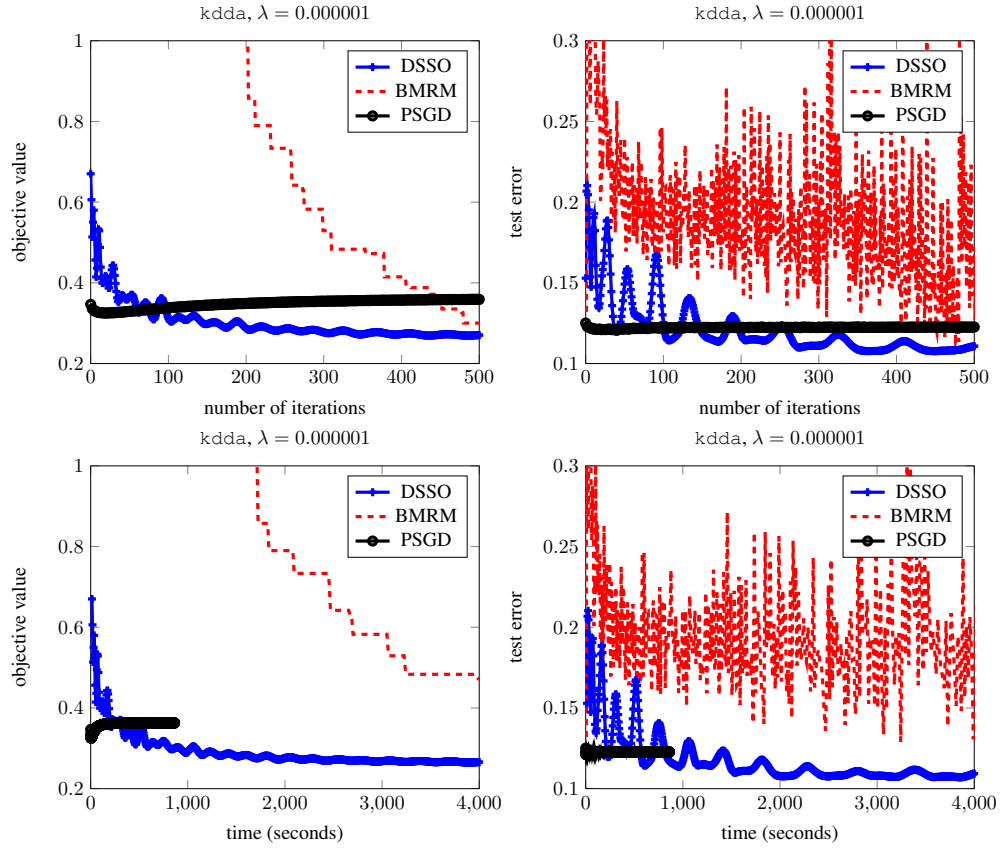


Figure 49: Parallel experiments on kdda dataset with logistic loss. Regularization parameter was set to be 0.000001. We used 4 machines with utilizing 8 cores on each of them. In top figures the x -axis is the number of iterations, while in bottom figures it is the time spent. On the left, the y -axis is the objective value, while on the right it is the test error.

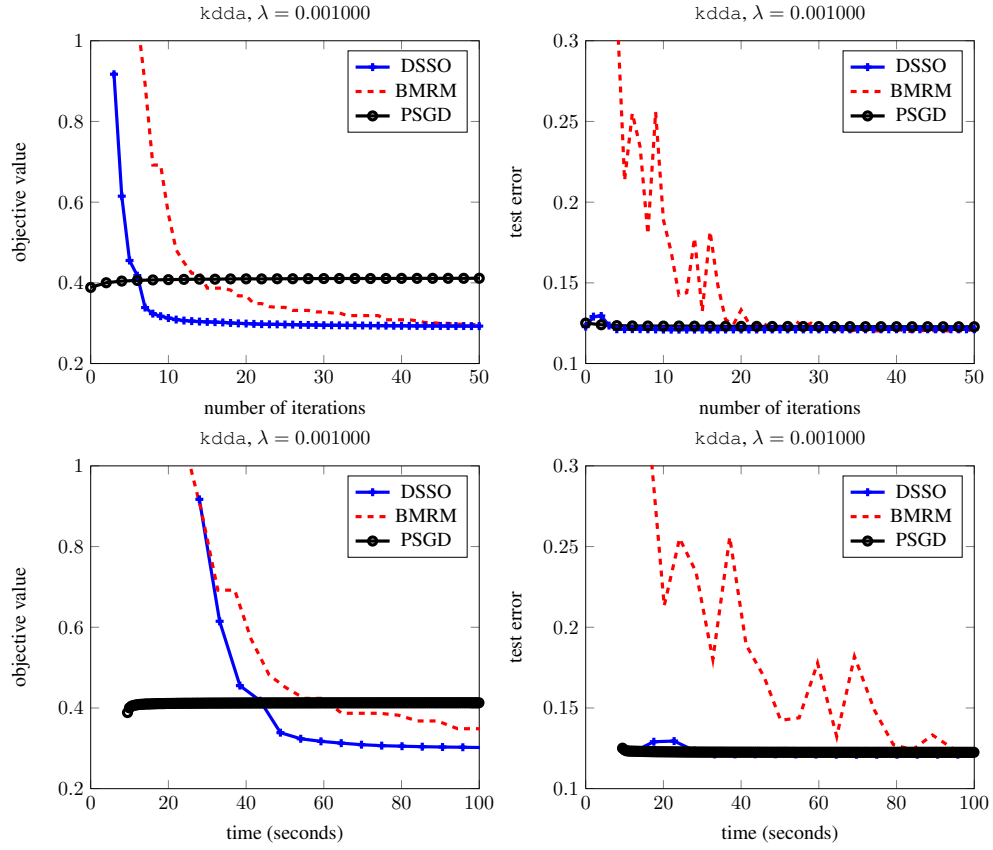


Figure 50: Parallel experiments on kdda dataset with svm loss. Regularization parameter was set to be 0.001000. We used 4 machines with utilizing 8 cores on each of them. In top figures the x -axis is the number of iterations, while in bottom figures it is the time spent. On the left, the y -axis is the objective value, while on the right it is the test error.

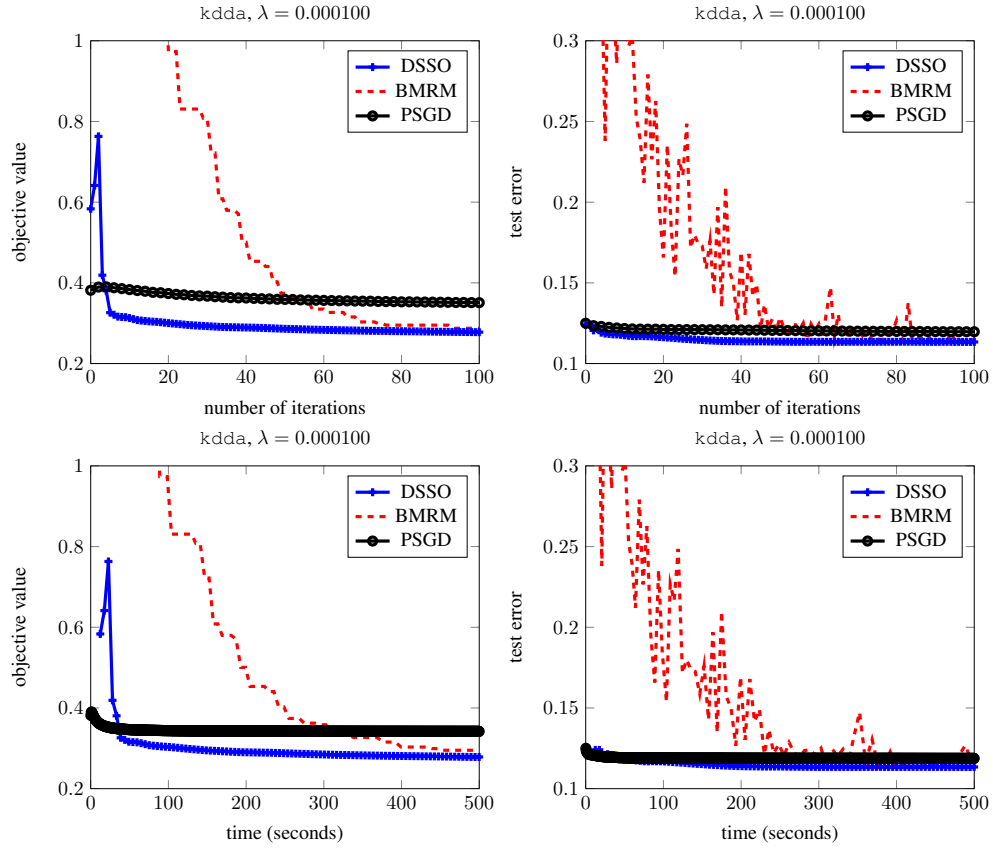


Figure 51: Parallel experiments on kdda dataset with svm loss. Regularization parameter was set to be 0.000100. We used 4 machines with utilizing 8 cores on each of them. In top figures the x -axis is the number of iterations, while in bottom figures it is the time spent. On the left, the y -axis is the objective value, while on the right it is the test error.

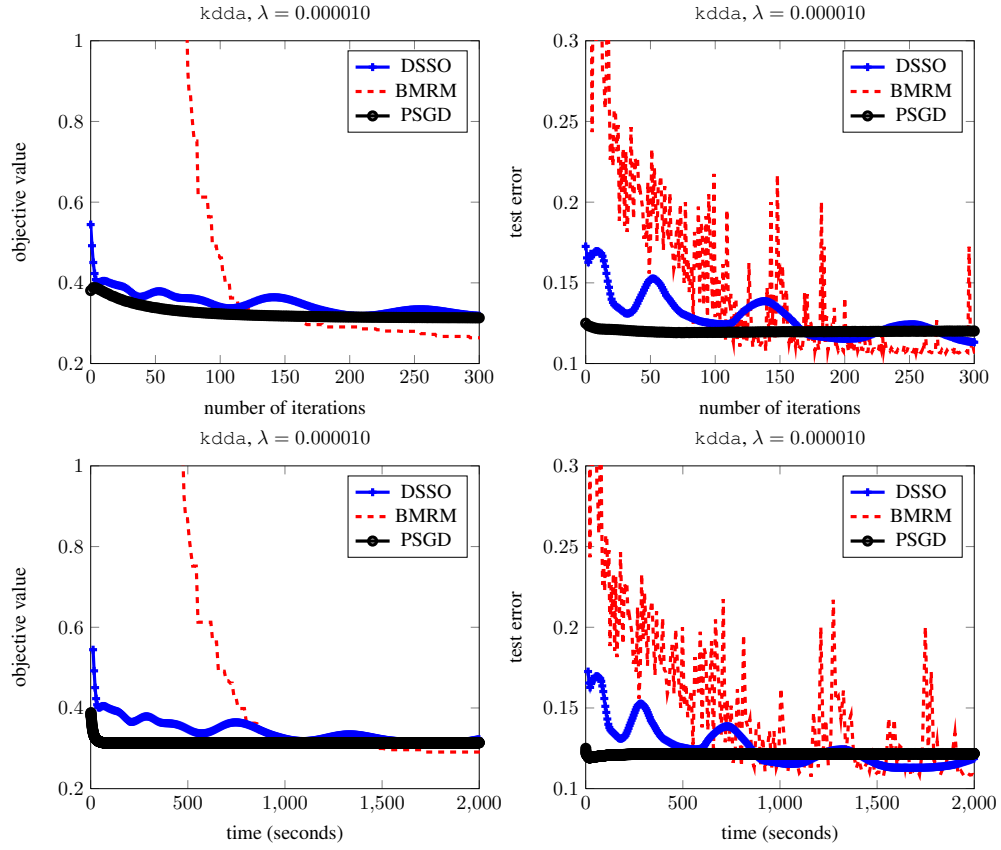


Figure 52: Parallel experiments on kdda dataset with svm loss. Regularization parameter was set to be 0.000010. We used 4 machines with utilizing 8 cores on each of them. In top figures the x -axis is the number of iterations, while in bottom figures it is the time spent. On the left, the y -axis is the objective value, while on the right it is the test error.

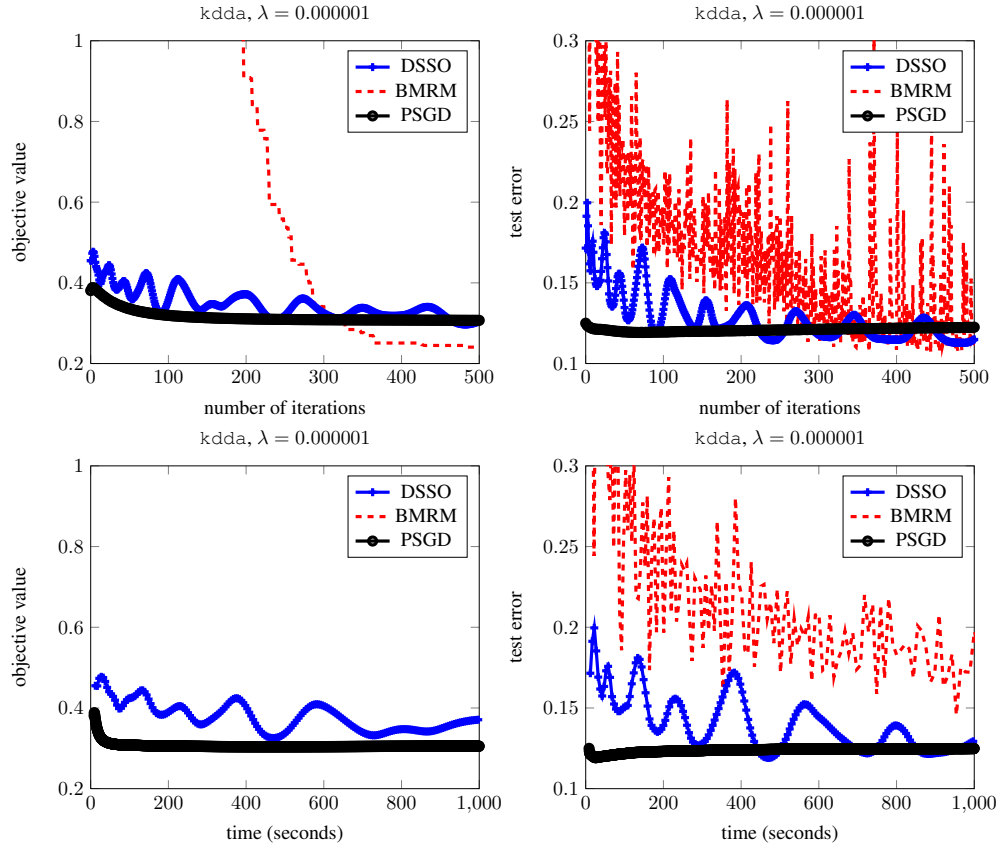


Figure 53: Parallel experiments on kdda dataset with svm loss. Regularization parameter was set to be 0.000001. We used 4 machines with utilizing 8 cores on each of them. In top figures the x -axis is the number of iterations, while in bottom figures it is the time spent. On the left, the y -axis is the objective value, while on the right it is the test error.

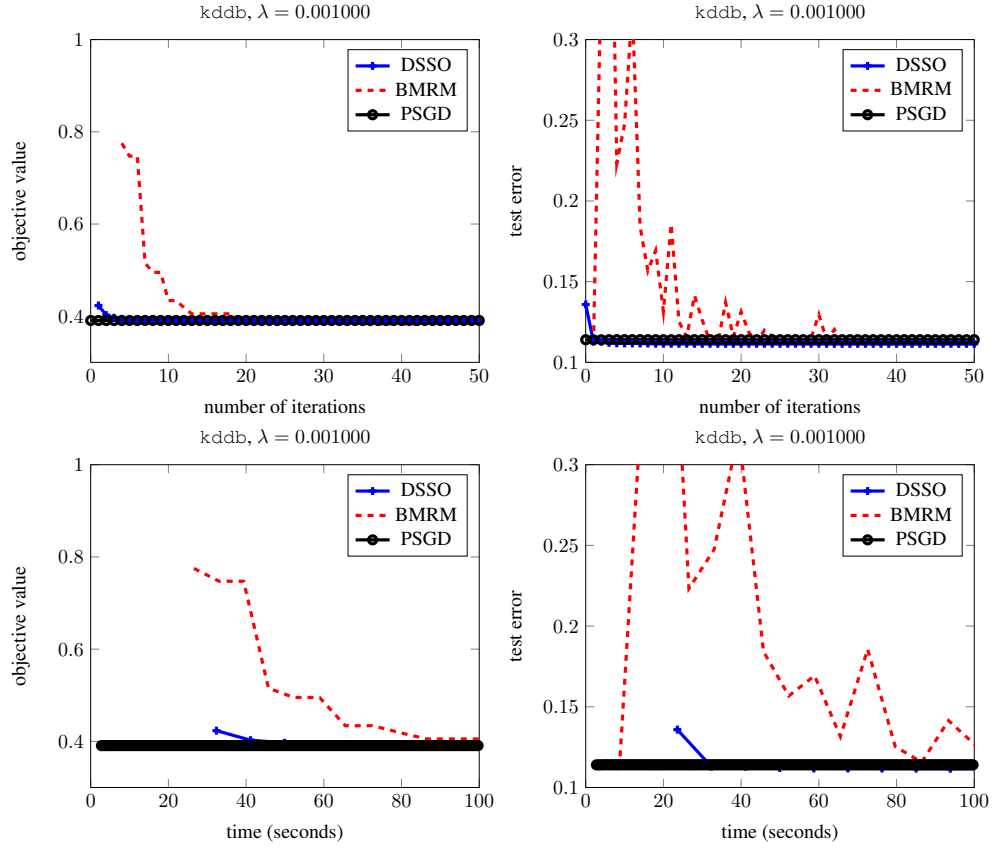


Figure 54: Parallel experiments on kddb dataset with logistic loss. Regularization parameter was set to be 0.001000. We used 4 machines with utilizing 8 cores on each of them. In top figures the x -axis is the number of iterations, while in bottom figures it is the time spent. On the left, the y -axis is the objective value, while on the right it is the test error.

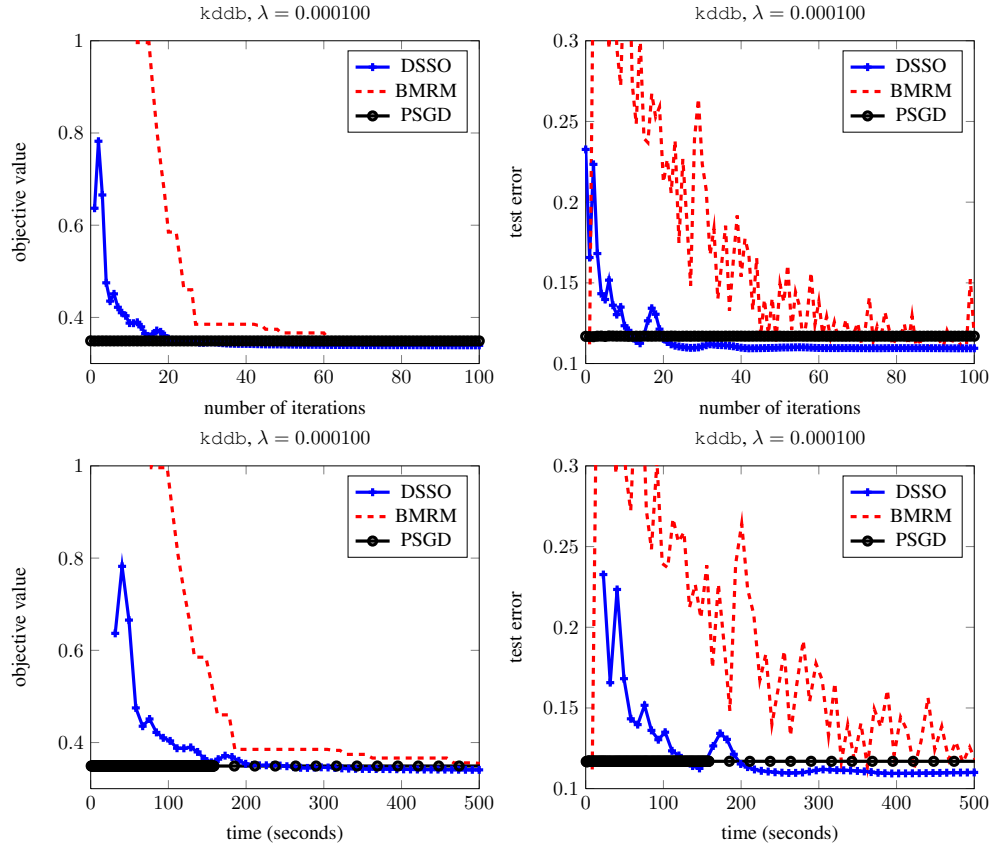


Figure 55: Parallel experiments on kddb dataset with logistic loss. Regularization parameter was set to be 0.000100. We used 4 machines with utilizing 8 cores on each of them. In top figures the x -axis is the number of iterations, while in bottom figures it is the time spent. On the left, the y -axis is the objective value, while on the right it is the test error.

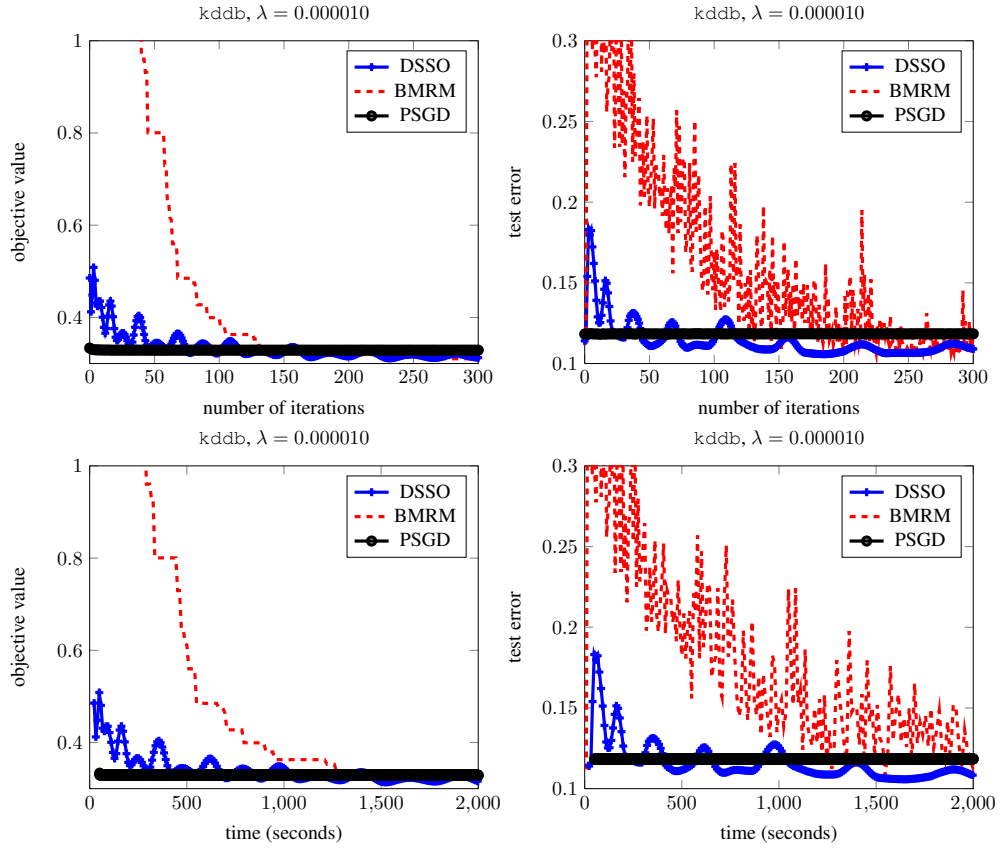


Figure 56: Parallel experiments on kddb dataset with logistic loss. Regularization parameter was set to be 0.000010. We used 4 machines with utilizing 8 cores on each of them. In top figures the x -axis is the number of iterations, while in bottom figures it is the time spent. On the left, the y -axis is the objective value, while on the right it is the test error.

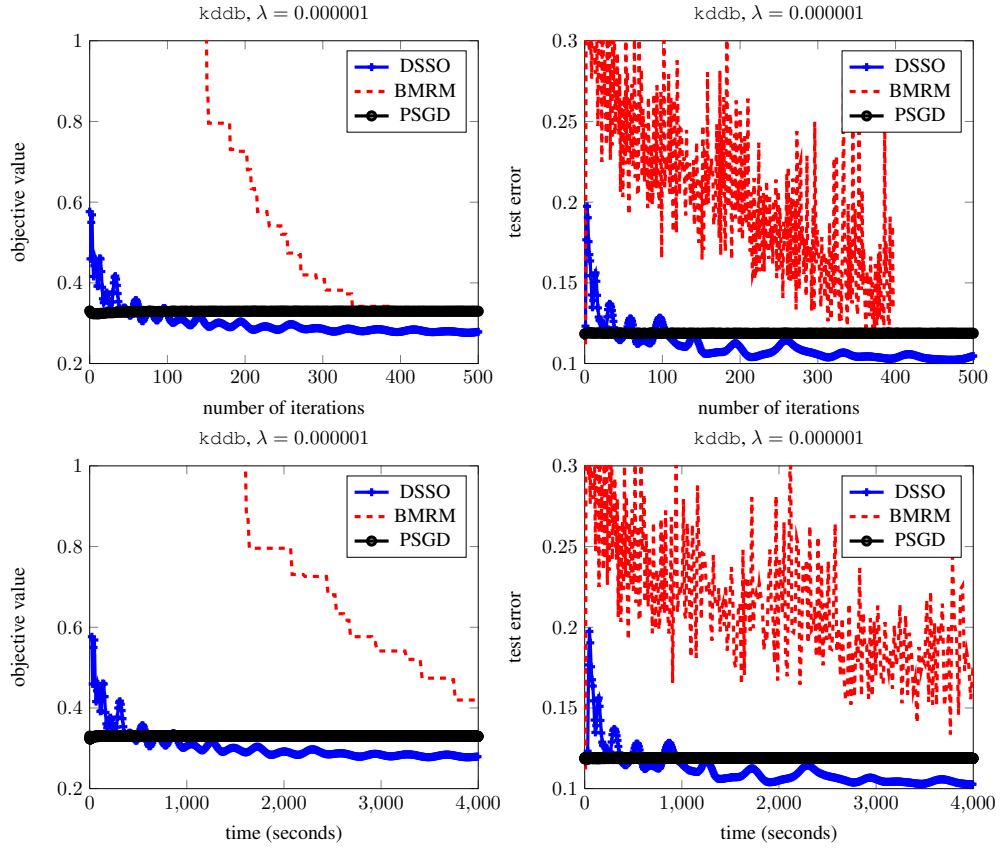


Figure 57: Parallel experiments on kddb dataset with logistic loss. Regularization parameter was set to be 0.000001. We used 4 machines with utilizing 8 cores on each of them. In top figures the x -axis is the number of iterations, while in bottom figures it is the time spent. On the left, the y -axis is the objective value, while on the right it is the test error.

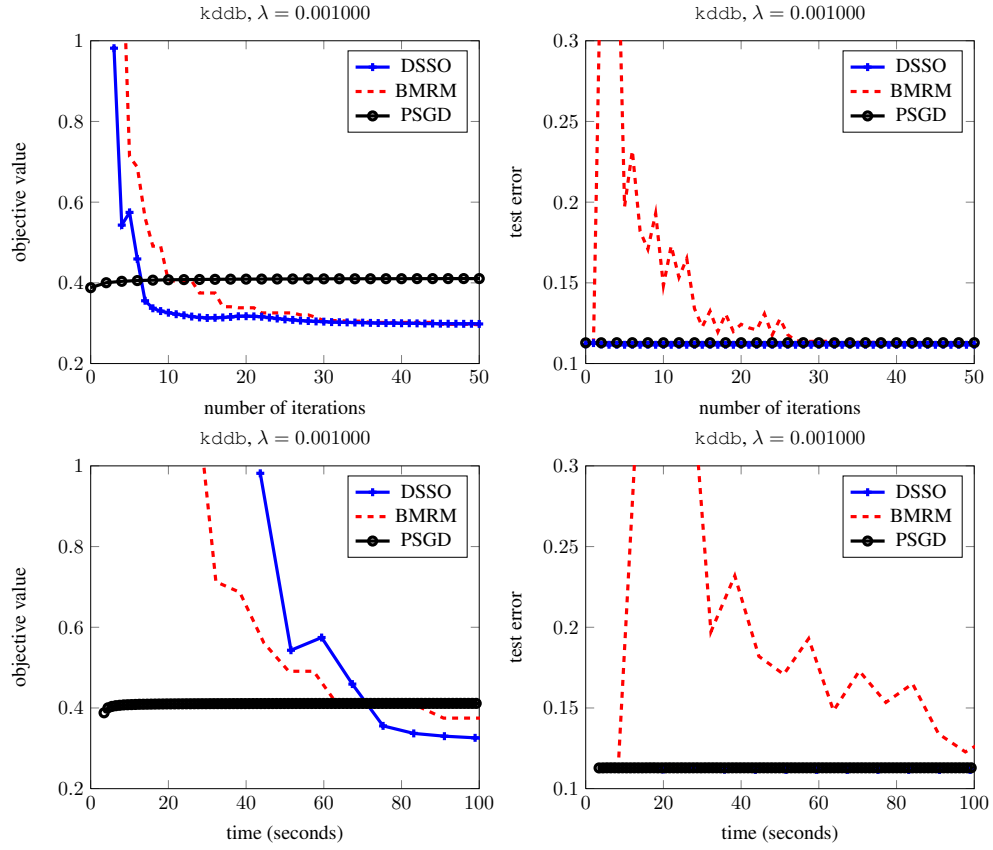


Figure 58: Parallel experiments on kddb dataset with svm loss. Regularization parameter was set to be 0.001000. We used 4 machines with utilizing 8 cores on each of them. In top figures the x -axis is the number of iterations, while in bottom figures it is the time spent. On the left, the y -axis is the objective value, while on the right it is the test error.

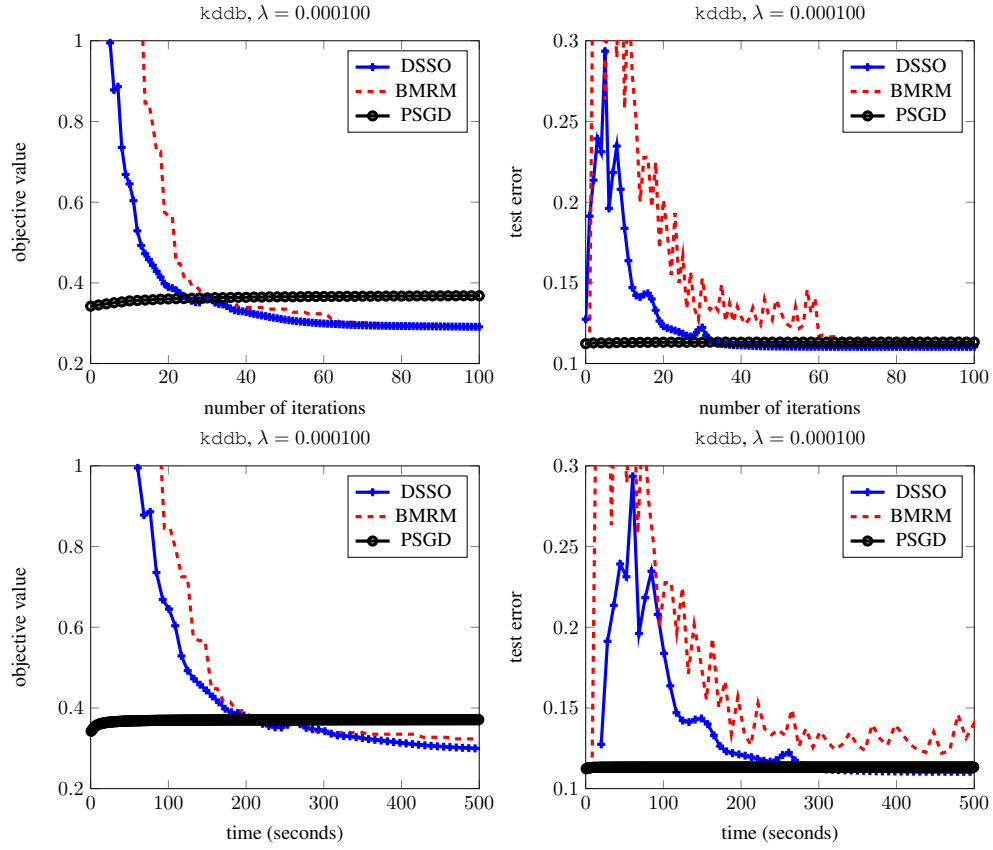


Figure 59: Parallel experiments on kddb dataset with svm loss. Regularization parameter was set to be 0.000100. We used 4 machines with utilizing 8 cores on each of them. In top figures the x -axis is the number of iterations, while in bottom figures it is the time spent. On the left, the y -axis is the objective value, while on the right it is the test error.

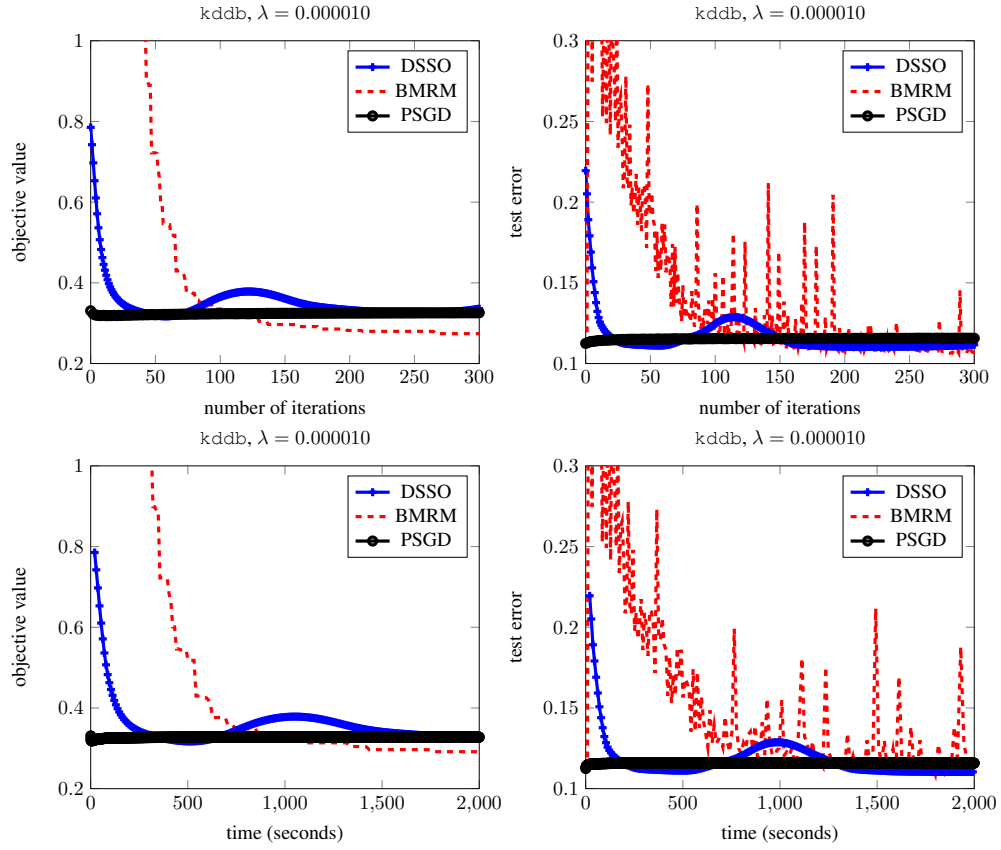


Figure 60: Parallel experiments on kddb dataset with svm loss. Regularization parameter was set to be 0.000010. We used 4 machines with utilizing 8 cores on each of them. In top figures the x -axis is the number of iterations, while in bottom figures it is the time spent. On the left, the y -axis is the objective value, while on the right it is the test error.

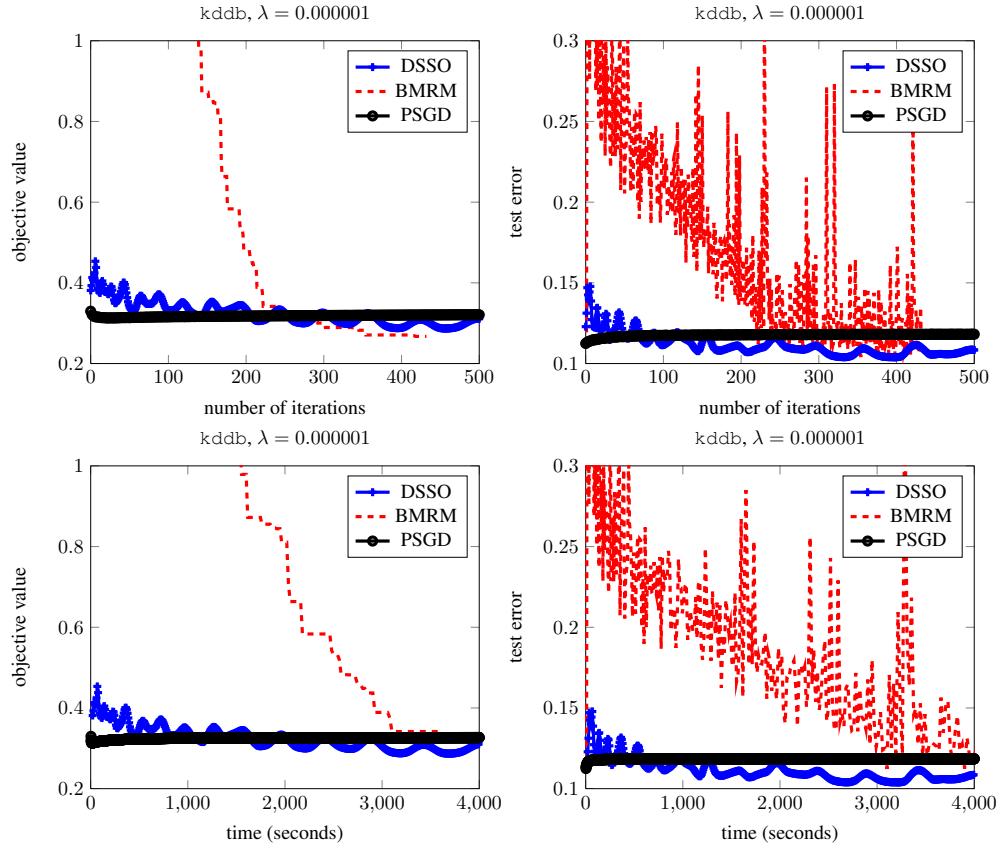


Figure 61: Parallel experiments on kddb dataset with svm loss. Regularization parameter was set to be 0.000001. We used 4 machines with utilizing 8 cores on each of them. In top figures the x -axis is the number of iterations, while in bottom figures it is the time spent. On the left, the y -axis is the objective value, while on the right it is the test error.

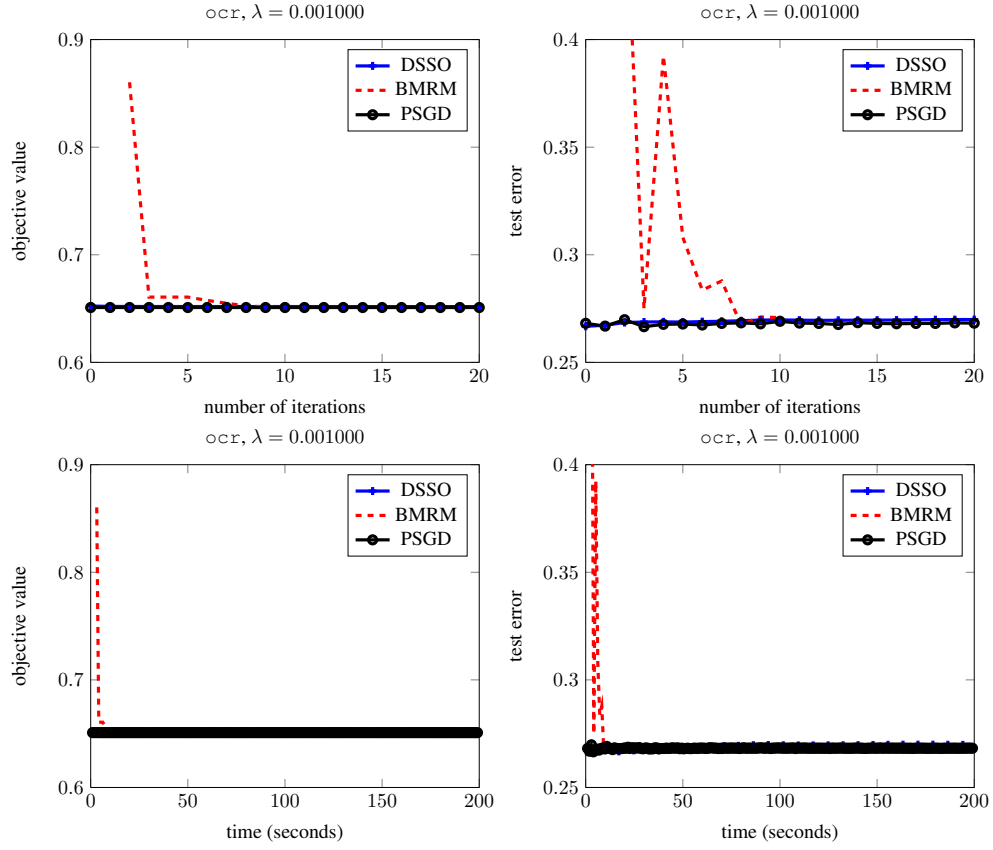


Figure 62: Parallel experiments on ocr dataset with logistic loss. Regularization parameter was set to be 0.001000. We used 4 machines with utilizing 8 cores on each of them. In top figures the x -axis is the number of iterations, while in bottom figures it is the time spent. On the left, the y -axis is the objective value, while on the right it is the test error.

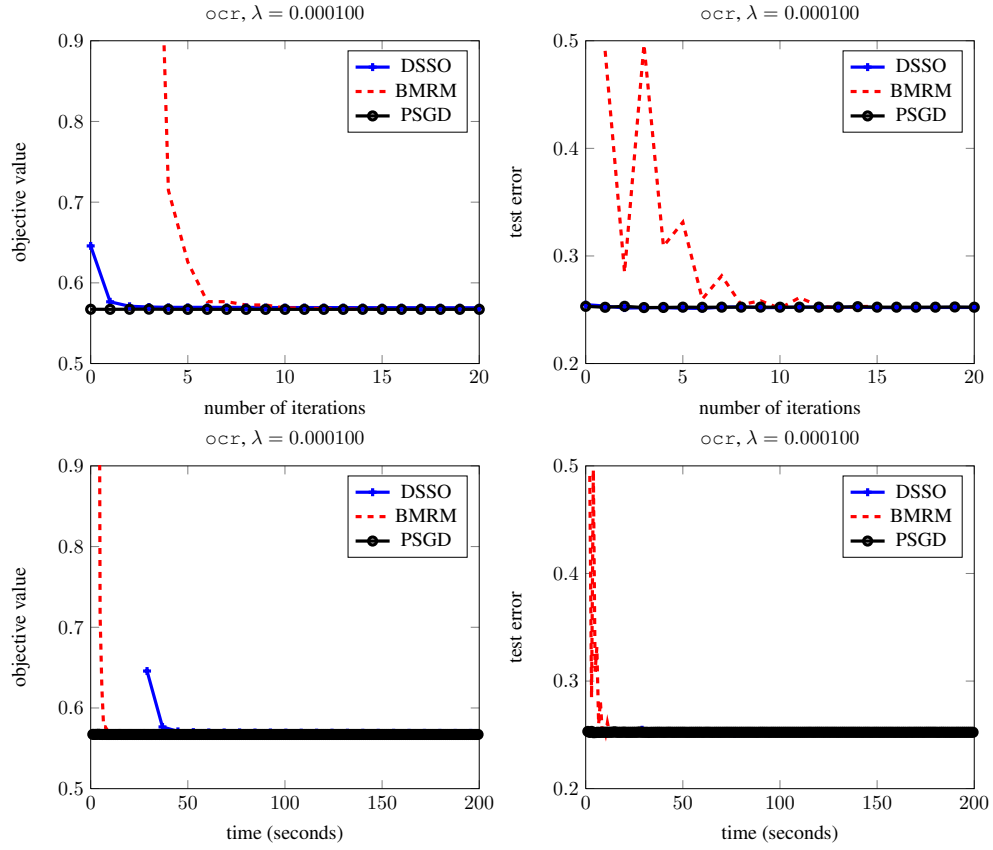


Figure 63: Parallel experiments on ocr dataset with logistic loss. Regularization parameter was set to be 0.000100. We used 4 machines with utilizing 8 cores on each of them. In top figures the x -axis is the number of iterations, while in bottom figures it is the time spent. On the left, the y -axis is the objective value, while on the right it is the test error.

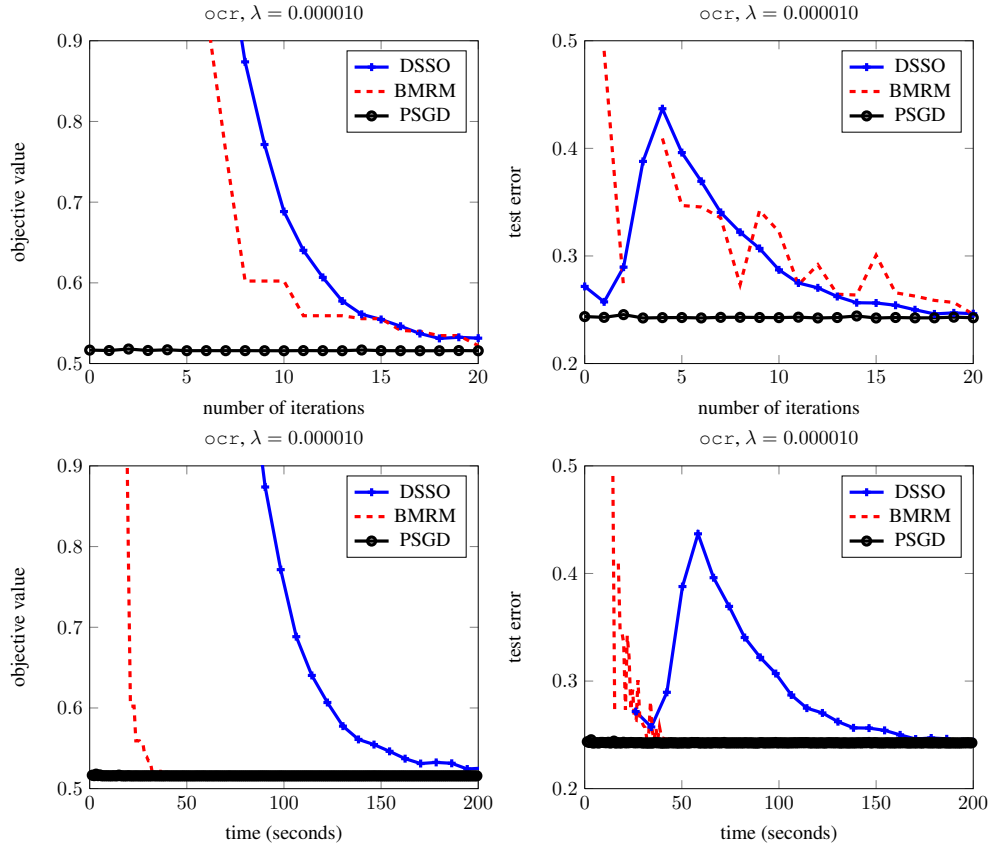


Figure 64: Parallel experiments on ocr dataset with logistic loss. Regularization parameter was set to be 0.000010. We used 4 machines with utilizing 8 cores on each of them. In top figures the x -axis is the number of iterations, while in bottom figures it is the time spent. On the left, the y -axis is the objective value, while on the right it is the test error.

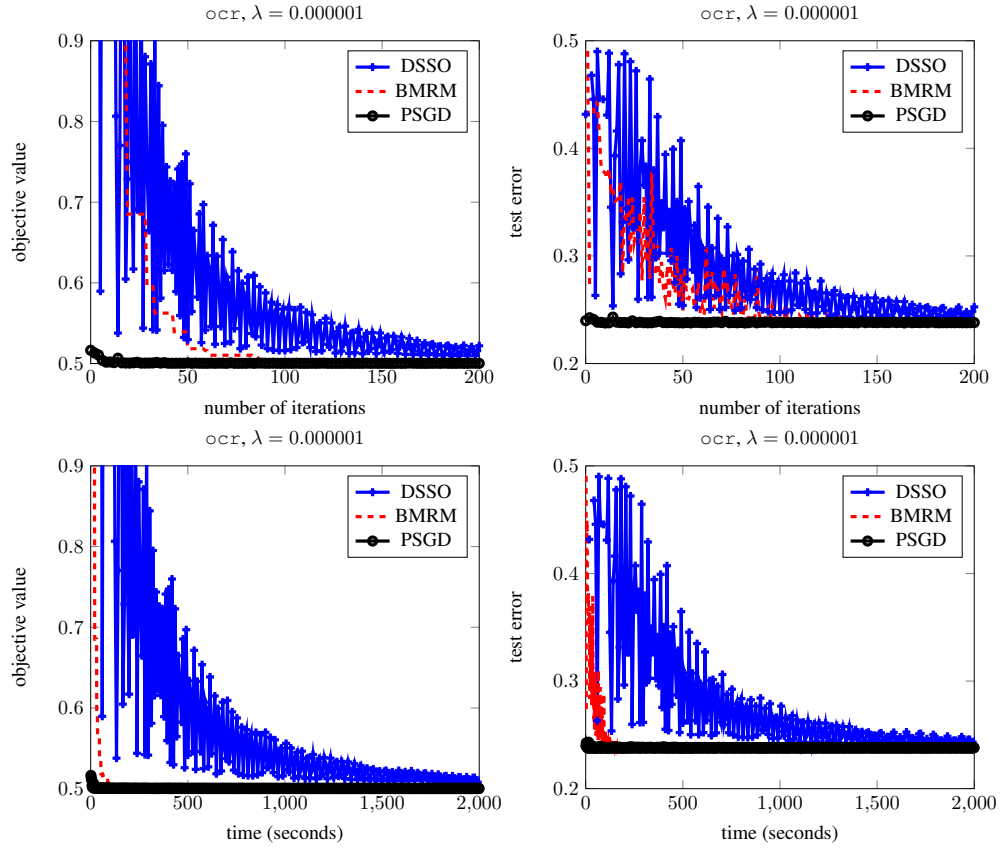


Figure 65: Parallel experiments on ocr dataset with logistic loss. Regularization parameter was set to be 0.000001. We used 4 machines with utilizing 8 cores on each of them. In top figures the x -axis is the number of iterations, while in bottom figures it is the time spent. On the left, the y -axis is the objective value, while on the right it is the test error.

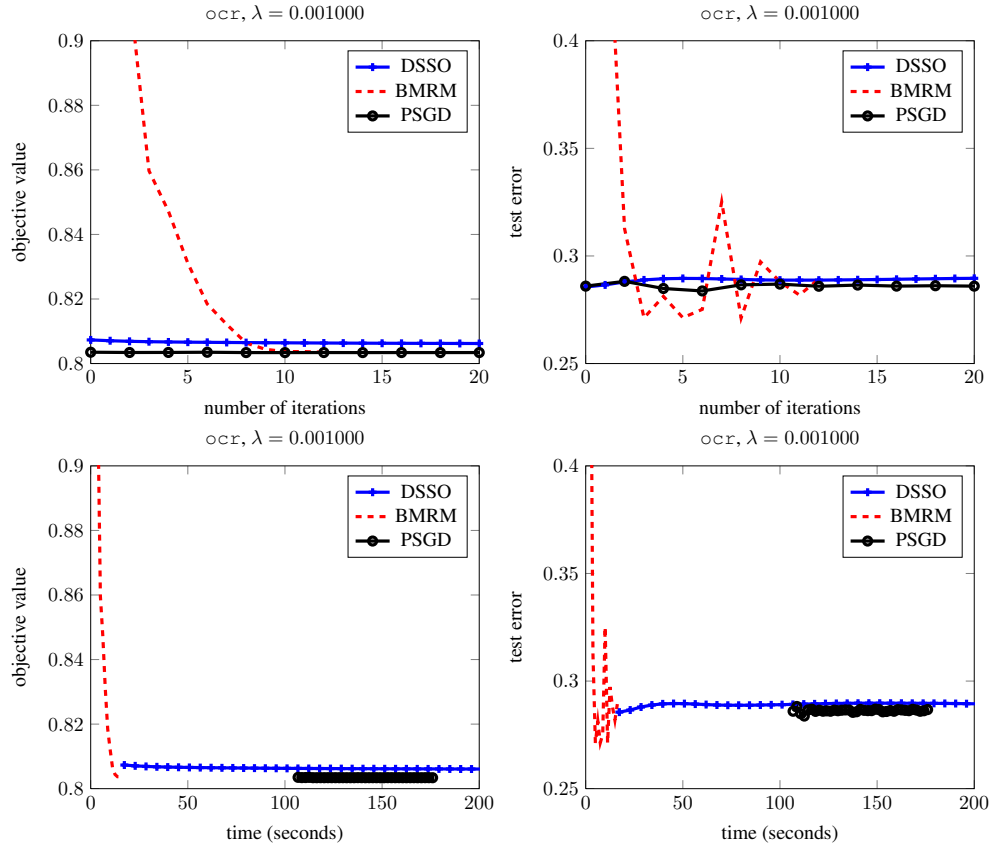


Figure 66: Parallel experiments on ocr dataset with svm loss. Regularization parameter was set to be 0.001000. We used 4 machines with utilizing 8 cores on each of them. In top figures the x -axis is the number of iterations, while in bottom figures it is the time spent. On the left, the y -axis is the objective value, while on the right it is the test error.

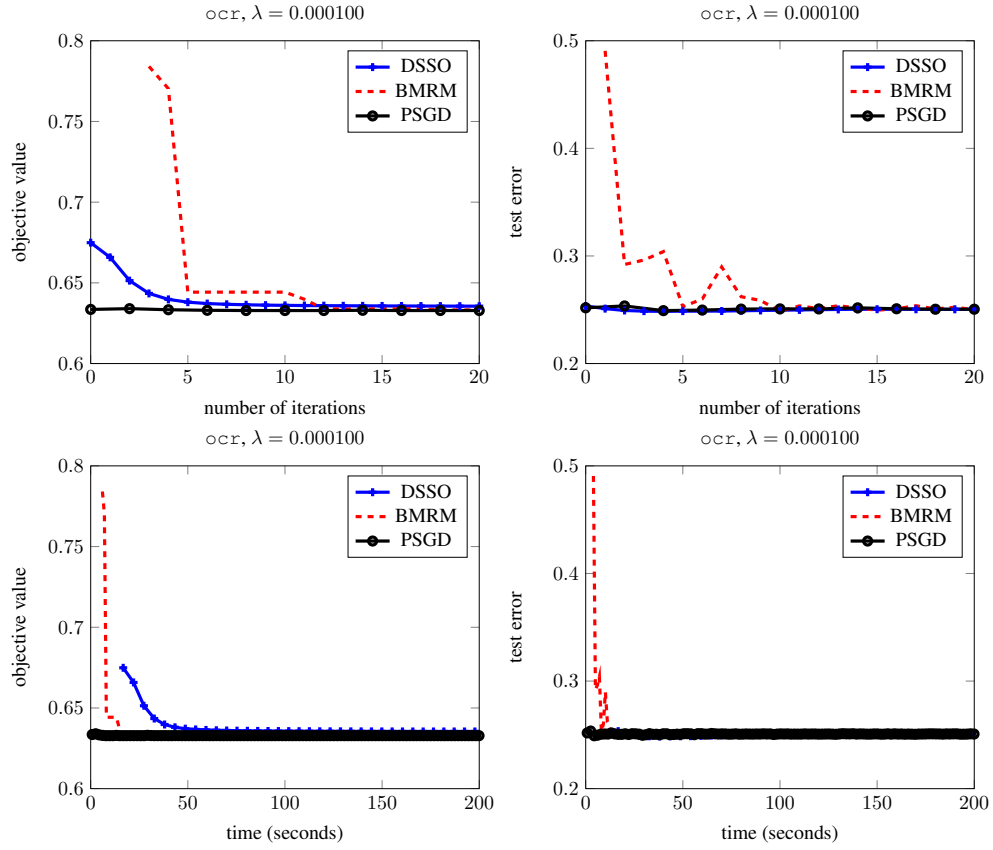


Figure 67: Parallel experiments on ocr dataset with svm loss. Regularization parameter was set to be 0.000100. We used 4 machines with utilizing 8 cores on each of them. In top figures the x -axis is the number of iterations, while in bottom figures it is the time spent. On the left, the y -axis is the objective value, while on the right it is the test error.

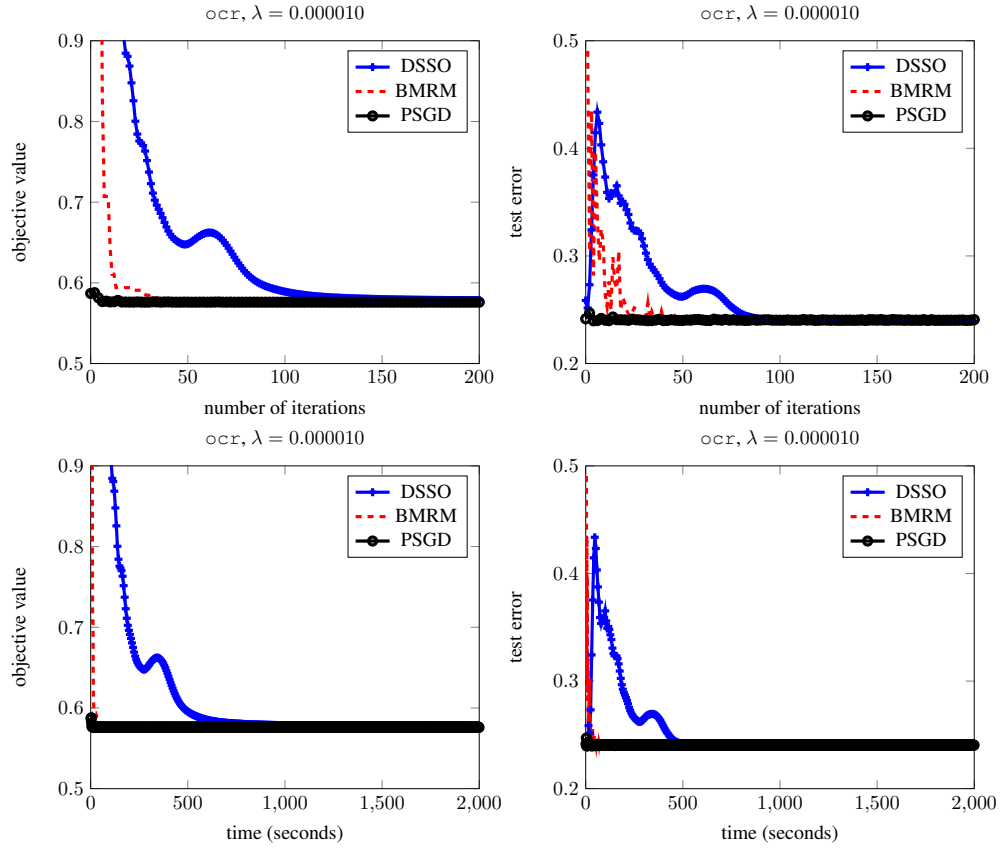


Figure 68: Parallel experiments on ocr dataset with svm loss. Regularization parameter was set to be 0.000010. We used 4 machines with utilizing 8 cores on each of them. In top figures the x -axis is the number of iterations, while in bottom figures it is the time spent. On the left, the y -axis is the objective value, while on the right it is the test error.

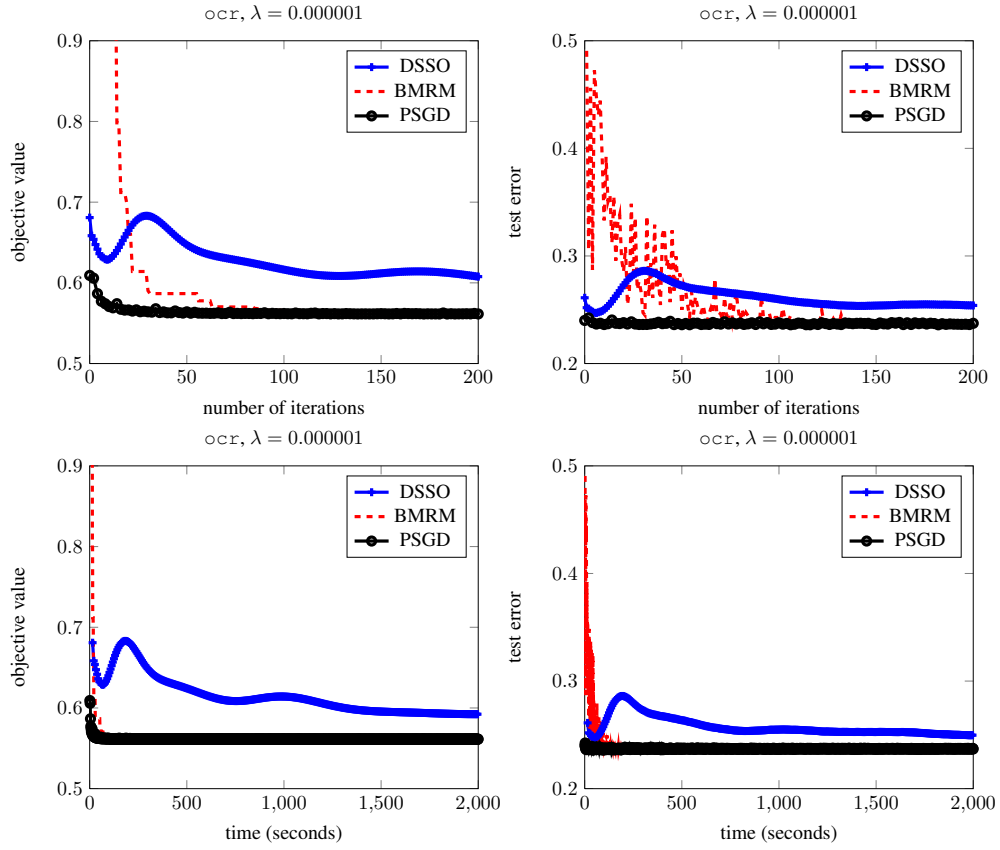


Figure 69: Parallel experiments on ocr dataset with svm loss. Regularization parameter was set to be 0.000001. We used 4 machines with utilizing 8 cores on each of them. In top figures the x -axis is the number of iterations, while in bottom figures it is the time spent. On the left, the y -axis is the objective value, while on the right it is the test error.

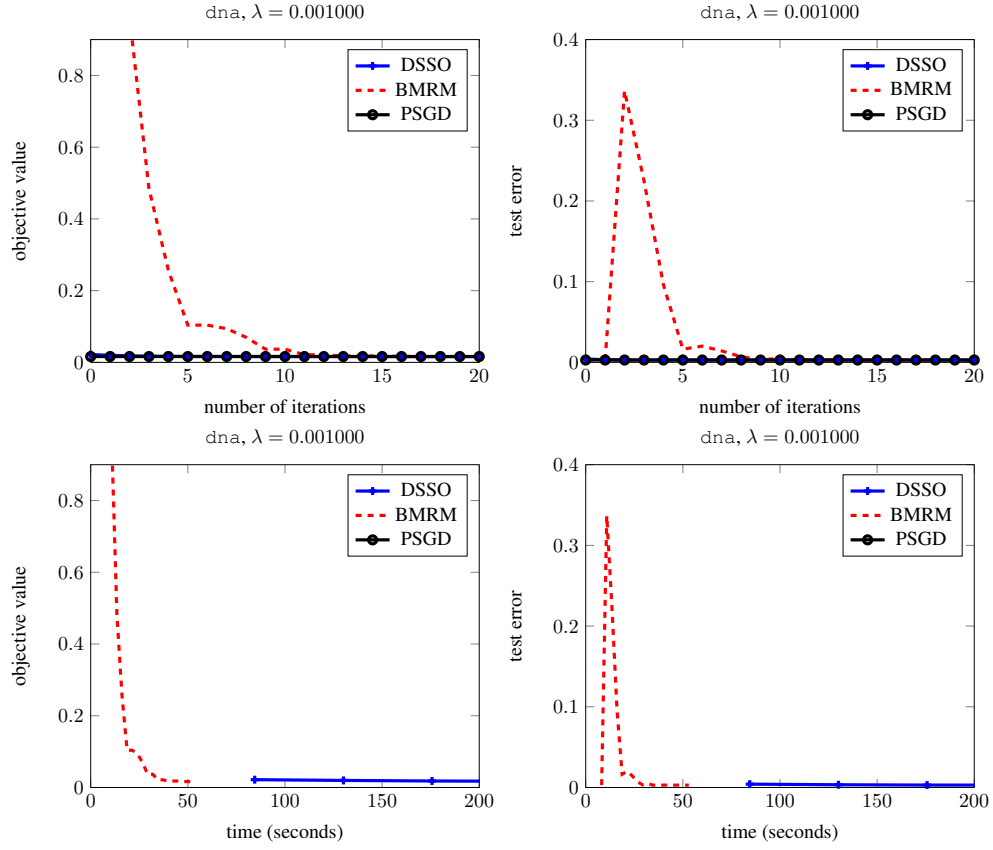


Figure 70: Parallel experiments on dna dataset with logistic loss. Regularization parameter was set to be 0.001000. We used 4 machines with utilizing 8 cores on each of them. In top figures the x -axis is the number of iterations, while in bottom it is the time spent. On the left, the y -axis is the objective value, while on the right it is the test error.

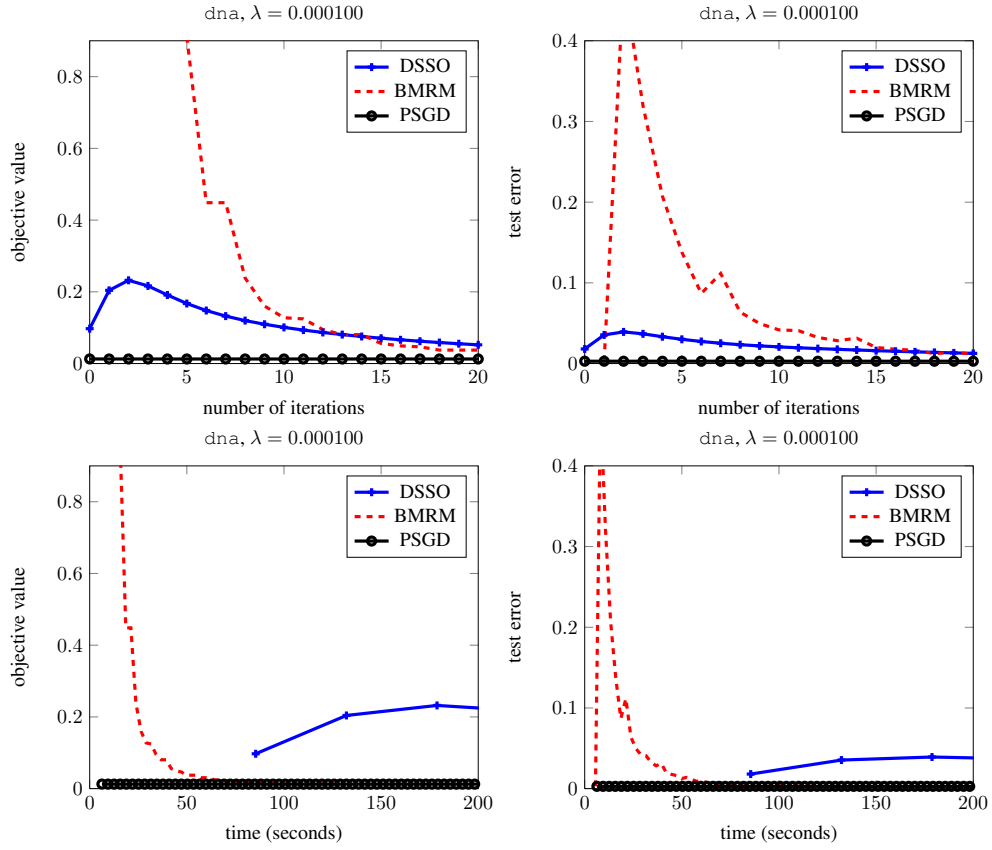


Figure 71: Parallel experiments on dna dataset with logistic loss. Regularization parameter was set to be 0.000100. We used 4 machines with utilizing 8 cores on each of them. In top figures the x -axis is the number of iterations, while in bottom it is the time spent. On the left, the y -axis is the objective value, while on the right it is the test error.

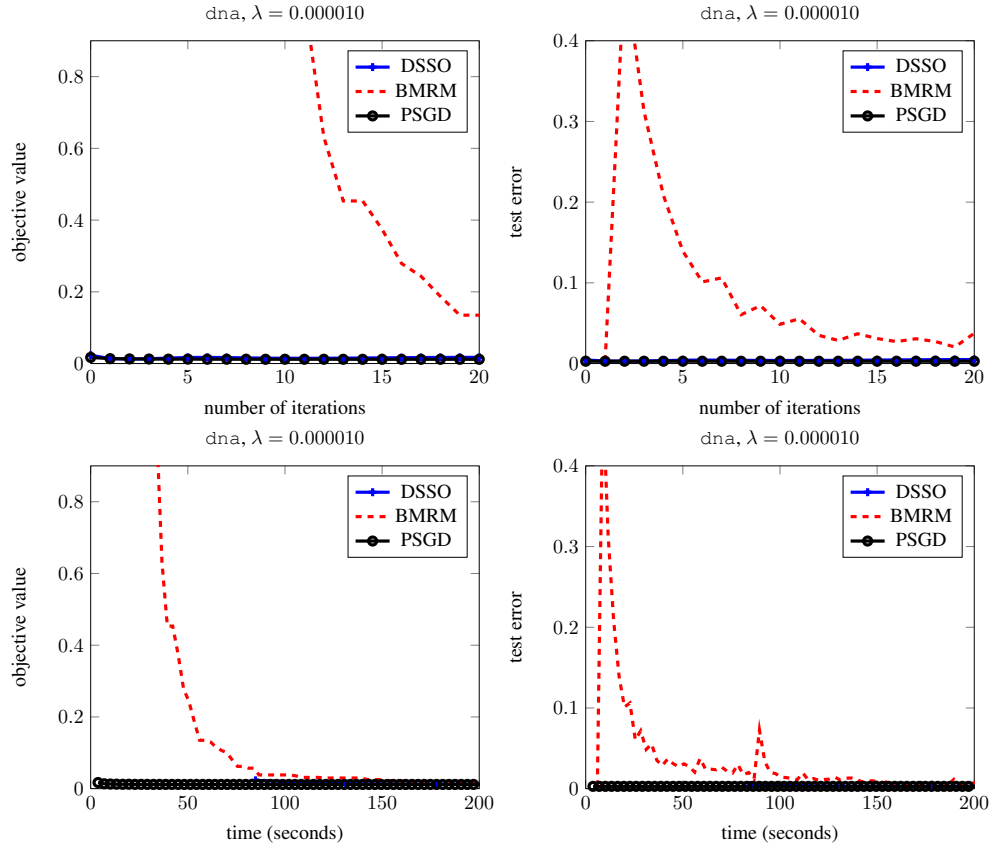


Figure 72: Parallel experiments on dna dataset with logistic loss. Regularization parameter was set to be 0.000010. We used 4 machines with utilizing 8 cores on each of them. In top figures the x -axis is the number of iterations, while in bottom it is the time spent. On the left, the y -axis is the objective value, while on the right it is the test error.

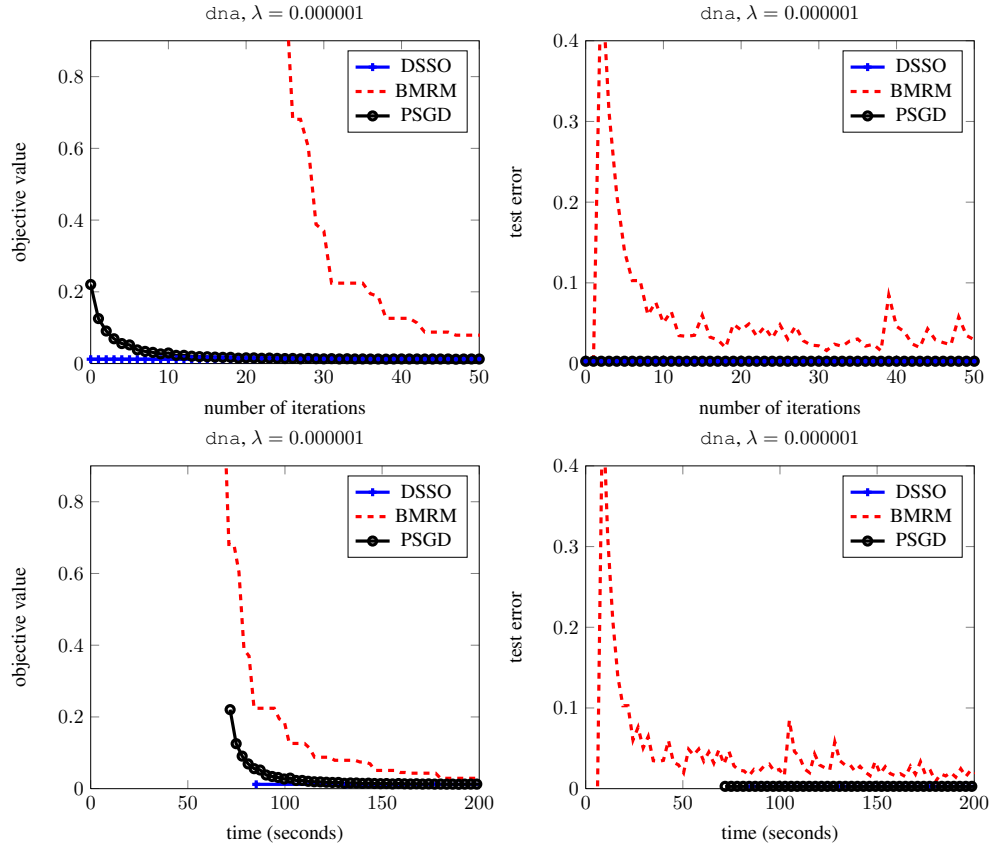


Figure 73: Parallel experiments on dna dataset with logistic loss. Regularization parameter was set to be 0.000001. We used 4 machines with utilizing 8 cores on each of them. In top figures the x -axis is the number of iterations, while in bottom it is the time spent. On the left, the y -axis is the objective value, while on the right it is the test error.

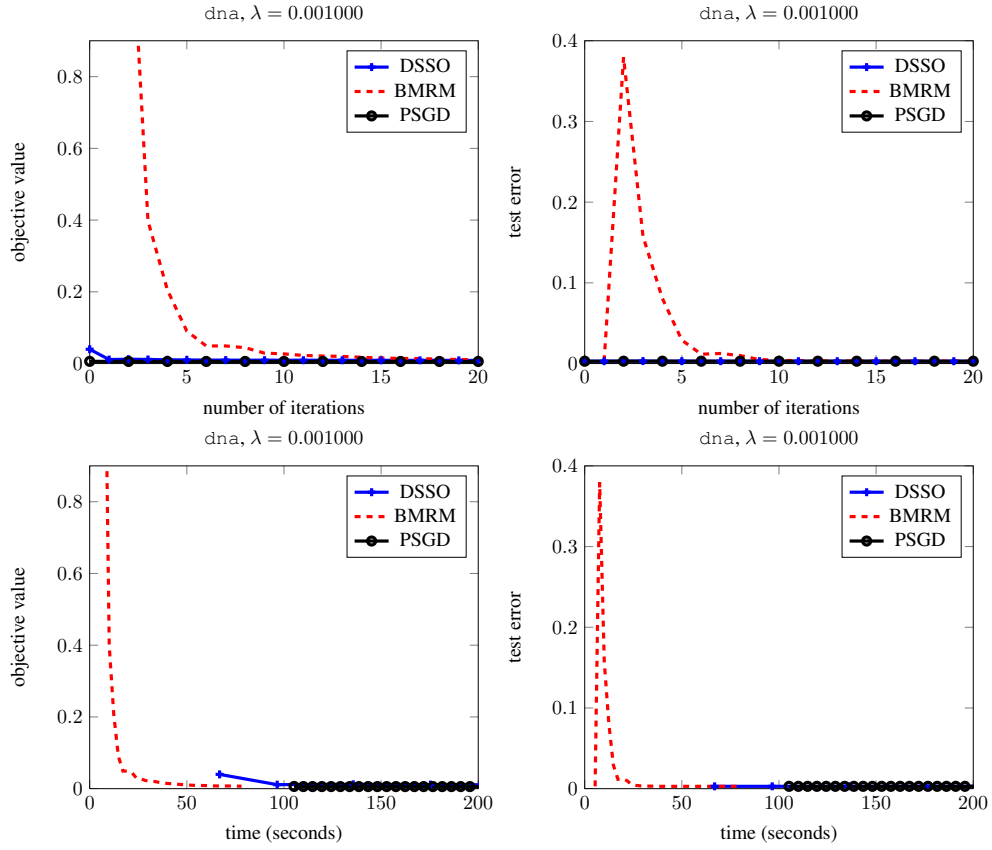


Figure 74: Parallel experiments on dna dataset with svm loss. Regularization parameter was set to be 0.001000. We used 4 machines with utilizing 8 cores on each of them. In top figures the x -axis is the number of iterations, while in bottom it is the time spent. On the left, the y -axis is the objective value, while on the right it is the test error.

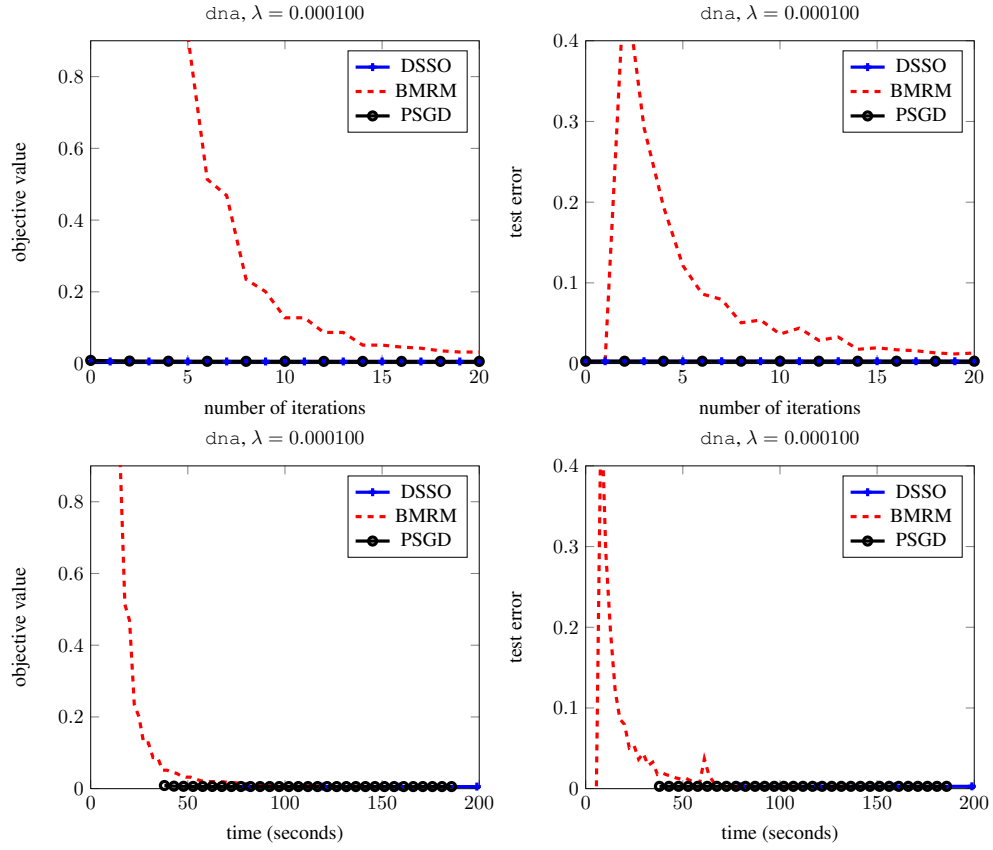


Figure 75: Parallel experiments on dna dataset with svm loss. Regularization parameter was set to be 0.000100. We used 4 machines with utilizing 8 cores on each of them. In top figures the x -axis is the number of iterations, while in bottom it is the time spent. On the left, the y -axis is the objective value, while on the right it is the test error.

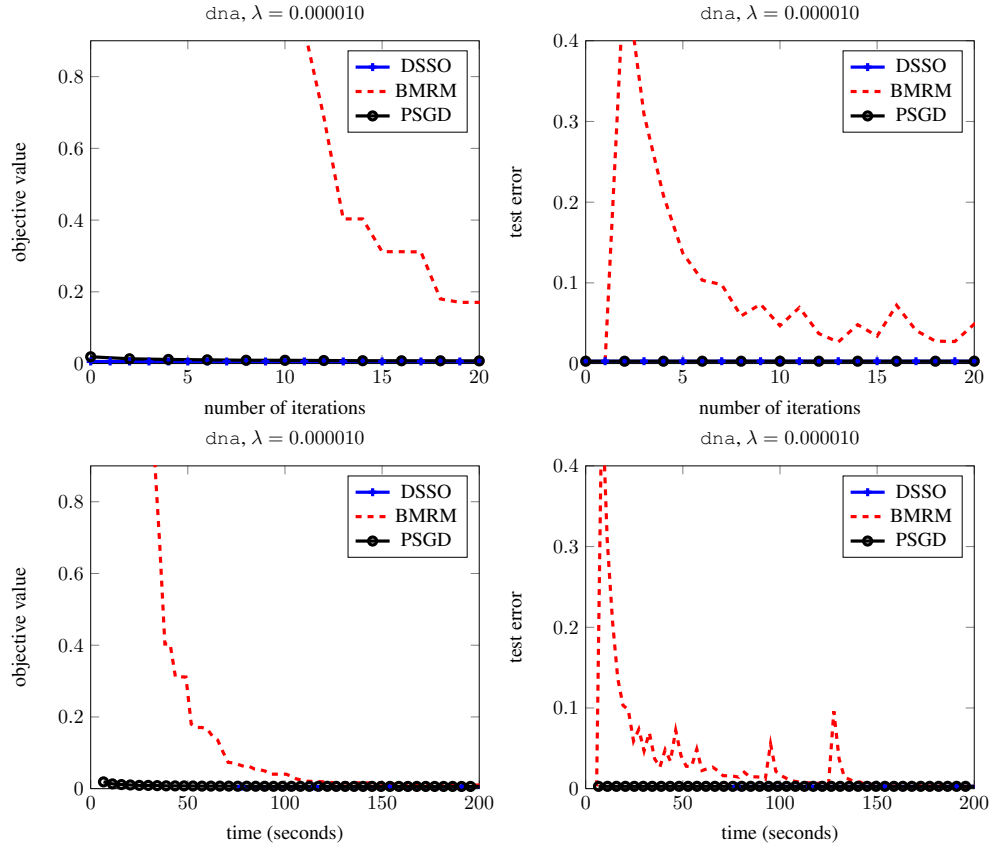


Figure 76: Parallel experiments on dna dataset with svm loss. Regularization parameter was set to be 0.000010. We used 4 machines with utilizing 8 cores on each of them. In top figures the x -axis is the number of iterations, while in bottom it is the time spent. On the left, the y -axis is the objective value, while on the right it is the test error.

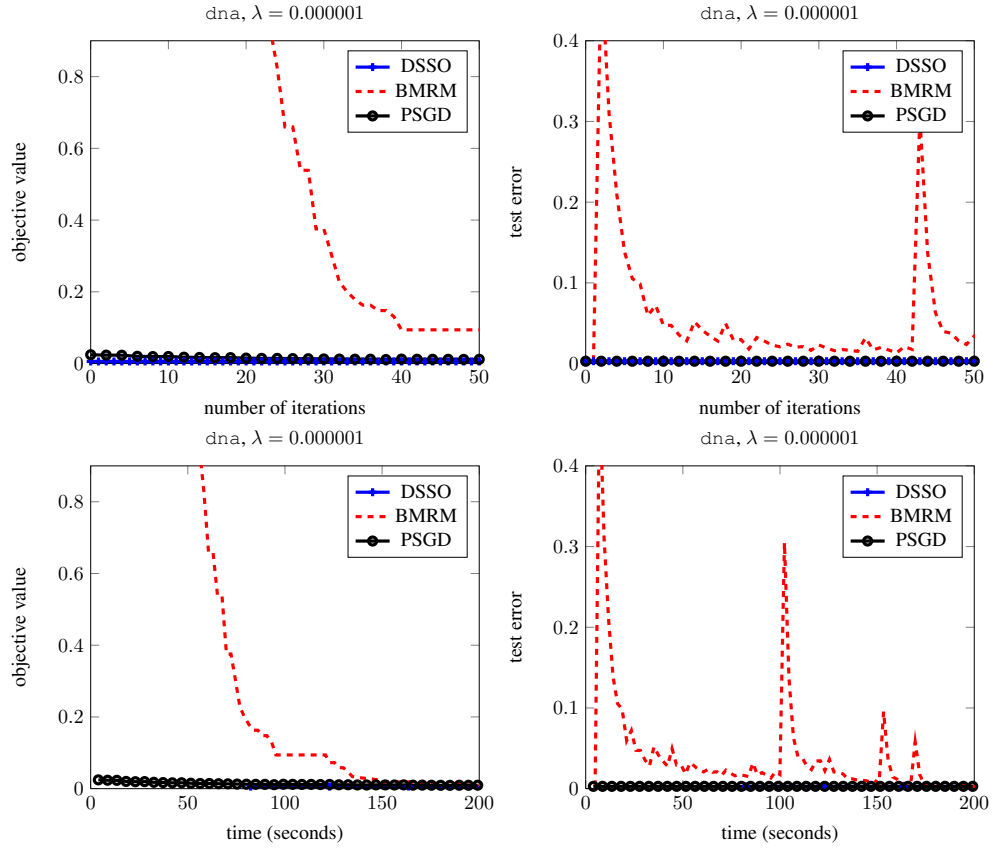


Figure 77: Parallel experiments on dna dataset with svm loss. Regularization parameter was set to be 0.000001. We used 4 machines with utilizing 8 cores on each of them. In top figures the x -axis is the number of iterations, while in bottom it is the time spent. On the left, the y -axis is the objective value, while on the right it is the test error.

F Additional Plot on Scaling

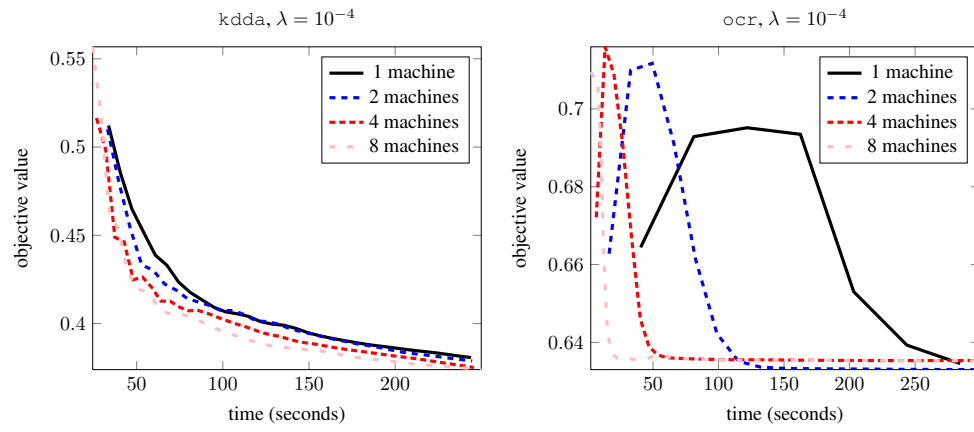


Figure 78: Convergence behavior of SVM on `ocr` with different number of machines. In each machine 8 cores were used.